

UNCLASSIFIED

AD NUMBER
AD452683
NEW LIMITATION CHANGE
TO Approved for public release, distribution unlimited
FROM Distribution authorized to U.S. Gov't. agencies and their contractors; Administrative/Operational Use; Nov 1964. Other requests shall be referred to Naval Engineering Lab., Port Hueneme, CA.
AUTHORITY
US Naval Construction Battalion Center ltr dtd 24 Oct 1974

THIS PAGE IS UNCLASSIFIED

UNCLASSIFIED

AD 4 5 2 6 8 3

DEFENSE DOCUMENTATION CENTER

FOR

SCIENTIFIC AND TECHNICAL INFORMATION

CAMERON STATION ALEXANDRIA, VIRGINIA



UNCLASSIFIED

NOTICE: When government or other drawings, specifications or other data are used for any purpose other than in connection with a definitely related government procurement operation, the U. S. Government thereby incurs no responsibility, nor any obligation whatsoever; and the fact that the Government may have formulated, furnished, or in any way supplied the said drawings, specifications, or other data is not to be regarded by implication or otherwise as in any manner licensing the holder or any other person or corporation, or conveying any rights or permission to manufacture, use or sell any patented invention that may in any way be related thereto.

CATALOGED BY DDG  
AS AD No. ~~452683~~

452683

DASA-13.018

**R 332**

Technical Report

STATIC AND BLAST LOADING  
OF SMALL BURIED CYLINDERS

10 November 1964



U. S. NAVAL CIVIL ENGINEERING LABORATORY  
Port Hueneme, California

DDC  
RECEIVED  
DEC 16 1964  
DDC-IRA C

FOR ERRATA

AD 4 5 2 6 8 3

THE FOLLOWING PAGES ARE CHANGES

TO BASIC DOCUMENT



U. S. NAVAL CIVIL ENGINEERING  
LABORATORY  
PORT HUENEME. CALIFORNIA 93041

IN REPLY REFER TO:

L36/OWL/jw

12 January 1965

MEMORANDUM

From: Publications Division  
To: Distribution List Addressees

Subj: TR-332; missing pages

1. Some of the pages of TR-332, "Static and Blast Loading of Small Buried Cylinders," by J. R. Allgood and H. L. Gill, were missing in the final printed copies. These pages have been rerun and are enclosed. If your copy is one with the missing pages, will you please insert the enclosed pages; if your copy is complete, please destroy the enclosure.

*Ocean W Lucas*

OCEAN W. LUCAS  
Director  
Publications Division

452683

*ADM 6200*

# STATIC AND BLAST LOADING OF SMALL BURIED CYLINDERS.

Y-F008-08-02-108, DASA-13.018

Type C

by

J. R. Allgood and H. L. Gill

## ABSTRACT

This research was performed to obtain information on the behavior of shallow-buried cylinders subjected to static and blast loads in support of the task objective of gaining knowledge to provide guidelines for developing design methods for underground protective structures. It was especially desired to obtain data on the time and space variations of deflection, thrust, and moment under the two types of loading for purposes of making a comparison.

The results show that the net arching across a flexible shallow-buried cylinder is small and that the maximum moment occurs at the bottom of the cylinder. Differences in response to static and blast loading are relatively small except for the crown, which deflects about twice as much under blast loading as under corresponding static loading. An analogy with the simple spring-mass system is drawn to explain this behavior. Information obtained on the influence of placing a low-strength isolating material in the soil over a cylinder indicates that such an expedient is of questionable benefit.

The complete significance of the test results can be appreciated only when correlated with other available test data and theory. Such a correlation is accomplished in a companion report.

Qualified requesters may obtain copies of this report from DDC.  
The Laboratory invites comment on this report, particularly on the  
results obtained by those who have applied the information.  
This work sponsored by the Defense Atomic Support Agency

## CONTENTS

	page
INTRODUCTION . . . . .	1
Subject and Purpose of Report . . . . .	1
Analysis of the Problem . . . . .	1
Review of Previous Work . . . . .	2
Approach and Scope . . . . .	3
EXPERIMENTAL WORK . . . . .	4
Loading Device . . . . .	4
Description of Soil-Structure System . . . . .	4
Instrumentation . . . . .	8
Recording Equipment . . . . .	8
Gas Pressure . . . . .	8
Strains . . . . .	10
Deflections . . . . .	10
Interface Pressures . . . . .	10
Accelerations . . . . .	10
Measurement Errors . . . . .	13
Test Program and Procedure . . . . .	13
Vibration Test — Cylinders Uncovered . . . . .	13
Backfill Test — Static Loadings . . . . .	13
Static Tests . . . . .	13
Backfill Test — Dynamic Loadings . . . . .	14
Vibration Pretest — Cylinders Covered . . . . .	14
Dynamic Tests . . . . .	14
Vibration Post-Test — Cylinders Covered . . . . .	14
RESULTS AND DISCUSSION . . . . .	14
Introduction . . . . .	14
Natural Period . . . . .	15
Backfill Tests . . . . .	15
Static Tests . . . . .	16

	page
Dynamic Tests . . . . .	30
Comparison of Static and Dynamic Response . . . . .	50
Recapitulation . . . . .	50
Deficiencies of Work . . . . .	51
FINDINGS AND CONCLUSIONS . . . . .	53
ACKNOWLEDGMENTS . . . . .	53
REFERENCES . . . . .	54
APPENDIXES	
A — Soil Placement and Properties . . . . .	55
B — Cylinder Isolation . . . . .	58

## INTRODUCTION

### Subject and Purpose of Report

The experiments reported here were directed at obtaining guidelines to aid in the design of hardened sites and underground structures. They were planned to study the response of shallow-buried cylinders under static and blast loading. The work was accomplished under Task Y-F008-08-02-108, "Studies of Soil-Structure Interaction," sponsored by the Defense Atomic Support Agency through the Bureau of Yards and Docks.

The specific objective of the experimental program was to obtain information on time and space variations of deflection, thrust, and moment, since at the time the tests were performed no such information was available in the literature. It also was desired to learn something of the pressure distribution at the soil-cylinder interface and of the dispersion of the surface load around the discontinuity produced by the structure in the soil field. A secondary objective was to investigate the influence of a mechanical shielding material on the behavior of a buried cylinder. The results, then, were intended to permit comparisons of the behavior of shielded and unshielded cylinders under static and dynamic loads. Ultimately it was hoped that the information obtained would aid in the selection of assumptions and provide experimental data for substantiation of theoretical methods that would enable economical designs for underground protective structures.

### Analysis of the Problem

Thin-walled cylinders are known to be capable of resisting very large loads when they are buried in soil. They are ideally suited, therefore, to use as personnel shelters, as command and control centers, and for storage of critical materials and equipment to provide protection from nuclear attack. The difficulty in such use is that little is known about the exact nature of the behavior of cylinders in a soil environment. Empirical methods have been developed for culvert and pipeline design, but these methods are not adequate for the design of personnel structures where much larger loads occur than in normal culvert design and where human life is directly at stake.

To achieve sound design methods, it is necessary to understand the fundamental nature of the soil-interaction problem — to comprehend and to be able to predict such things as the form of the deflection, moment, and thrust distribution. One must also gain an understanding of the nature of the load transfer through the soil to the cylinder and of the character of the resistance provided by the soil as the cylinder deforms. Perhaps even more important is the requirement for knowing under what conditions buckling failure will occur.

Research work and field experience gained over the years have resulted in a general understanding of the phenomena of soil-structure interaction, but comprehension of the details of the action has remained deficient. For example, prior to completion of the tests described here, the distribution of moment and the exact nature of the deflection had not been obtained even under static load conditions. It was evident, therefore, that the first step to further understanding must involve extensive measurements on a model cylinder of sufficient size to ascertain that the true nature of response of the prototype would not be obscured.

Although the Navy's standard personnel shelter is an arch,<sup>1</sup> this study was undertaken because it was hypothesized that buried cylinders would make better shelters than buried arches in overpressure regions greater than 150 psi. In this overpressure region, ground shock is likely to be a major factor in design, and it is possible that a shock-isolated floor system might be more easily achieved in a cylinder than in an arch. Further, in the high overpressure regions, gross punching of an arch into the soil could destroy the water seals between the floor and the footing, thus permitting the intrusion of ground water. In a closed structure such as the cylinder, it should be much easier to maintain the watertight integrity. Previous tests, however, have demonstrated that punching of an arch in the soil permits the development of shear stresses in the soil and the transmission of a large percentage of the surface load across the structure by arching. Thus, it is evident that both the cylinder and the arch have advantages peculiar to their forms, and it behooves the designer to understand the advantages and disadvantages of each and where each may be best employed in providing protection.

#### Review of Previous Work

Considerable investigation has been conducted on thin-walled cylinders stemming from their use in highway and railroad beds. Most of this work has been semi-empirical in nature, after the philosophy that a rigorous analysis will remain impractical as long as there are imprecisely controlled variables in field installation and incomplete knowledge of soils. Recent requirements for underground shelters, however, have stimulated endeavors toward more precise understanding and analytical treatment.

A rather detailed review of previous work on hydrostatically loaded and buried cylinders is included in a companion report;<sup>2</sup> consequently, this material will not be repeated here.

The companion report presents a failure-plane analysis which gives (1) the minimum depth of cover required for all the surface load to be carried by arching, (2) the maximum percentage of surface load that can be carried by arching for any lesser depths, and (3) the relative defonation between a structure and the free field required to develop the maximum possible arching. Analysis of the possibility of collapse revealed that a cylinder may fail by elastic or inelastic action in the roof-caving and local transitional buckling modes in addition to failure through pure compression, joint failure, and excessive deflection. Evidence indicates that for depths of cover sufficient to provide radiation protection, and for relatively thin-walled cylinders, failure will normally be in the inelastic transitional mode where a local buckle develops at the bottom of the cylinder. Other aspects of the behavior of buried cylinders will be evident from the data and discussion presented here.

#### Approach and Scope

To fulfill the need for detailed information on behavior, experiments were designed to reveal the space and time variations of deflection, moment, and thrust under static and blast load conditions. They were not intended to obtain information on buckling for the reason that more tests would be required to define this type of failure than could be conducted. Further, the available loading equipment does not have sufficient capacity to produce failure in cylinders with diameter-to-thickness ratios and depths of cover of interest.

Design of the tests, consequently, was influenced largely by the available loading equipment, in addition to the desire to test as large a model as possible while keeping the cost within balance. A reasonably large model was deemed mandatory for the initial test to better insure that the behavior would be truly indicative of that of a full-sized prototype. For a large model system the number of tests that can be performed is restricted by the cost of controlled placement of large amounts of soil.

As a compromise of these factors, model structures with a span of one-tenth that of the intended prototype were used. Two contemporaneous cylinders were tested in each of the two series of tests, one cylinder with and one without a low-strength isolating material over the crown to compare the behavior with and without mechanical shielding. In Series I, the cylinders were tested statically; those in Series II were subjected to dynamic loads. Each setup was loaded several times. The system was idealized in that dry sand was used in the soil field and the dynamic loading was a plane wave rather than a traveling wave.

## EXPERIMENTAL WORK

### Loading Device

Both the static and the dynamic tests were performed in the test pit of the NCEL atomic blast simulator, as shown schematically in Figure 1. The blast simulator<sup>3</sup> is a device capable of developing chamber pressures from 0 to 185 psi with a rise time of 0.75 millisecond or greater and an exponential decay. The test pit beneath the simulator is 9 feet by 10 feet in plan and 12 feet deep. Skirt enclosures extending from the body of the simulator to the pit form a closed chamber where dynamic overpressures up to 25 psi may be applied to 90 square feet of surface area when the pit is filled with soil.

Uniformly distributed static loads are applied to the surface of the soil mass by inflating a pneumatic bag made of neoprene. This bag, 2 inches thick and essentially of the same plan dimensions as the test pit, reacts against the blast simulator through a timber planking and steel beam framework as shown in Figure 2. The bag is pressurized with nitrogen gas from a standard cylinder controlled with a precision pressure-calibrating unit to provide the desired surface loading.

### Description of Soil-Structure System

Although the loading assembly was different for the static and dynamic tests, the test setup was otherwise nearly identical for the two types of loading. The primary difference in the two was that the depth of soil below the structures was approximately 3 feet greater for the static tests than for the dynamic tests — about 9 feet for the static tests and about 6 feet for the dynamic.

The soil field consisted of dry sand compacted to a uniform density. This is the same material used in several previous soil-structure experiments at NCEL.<sup>4,5</sup> Prior to the installation of the cylinders in the test pit, the sand was placed in the pit to the designed elevation of the bottom of the cylinders. The soil placement procedure and the properties of the soil in place are described in Appendix A.

A view of the models braced in position prior to placement of the backfill is shown in Figure 3. The setup consisted of two cylinders 24 inches in diameter and 30 inches long placed end to end in such a manner as to act independently of each other and the end walls. The end walls were held apart by steel angles acting as columns, placed interior to the cylinders. The shells were rolled from galvanized sheet steel with a thickness of 0.0478 inch, and the ends were seam-welded. Physical properties of the cylinders are given in Table I. The seam weld was located at the center of the upper quadrant (45 degrees from vertical) opposite the instrumentation so that the weld would have the least influence on the response of the cylinder.

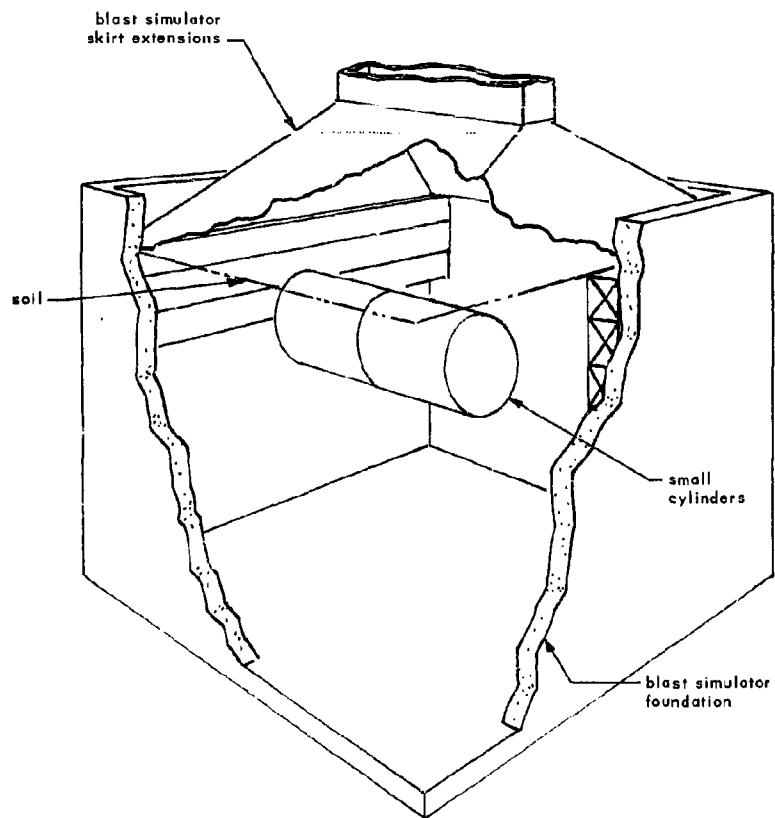


Figure 1. Perspective of blast simulator pit showing small buried cylinders.

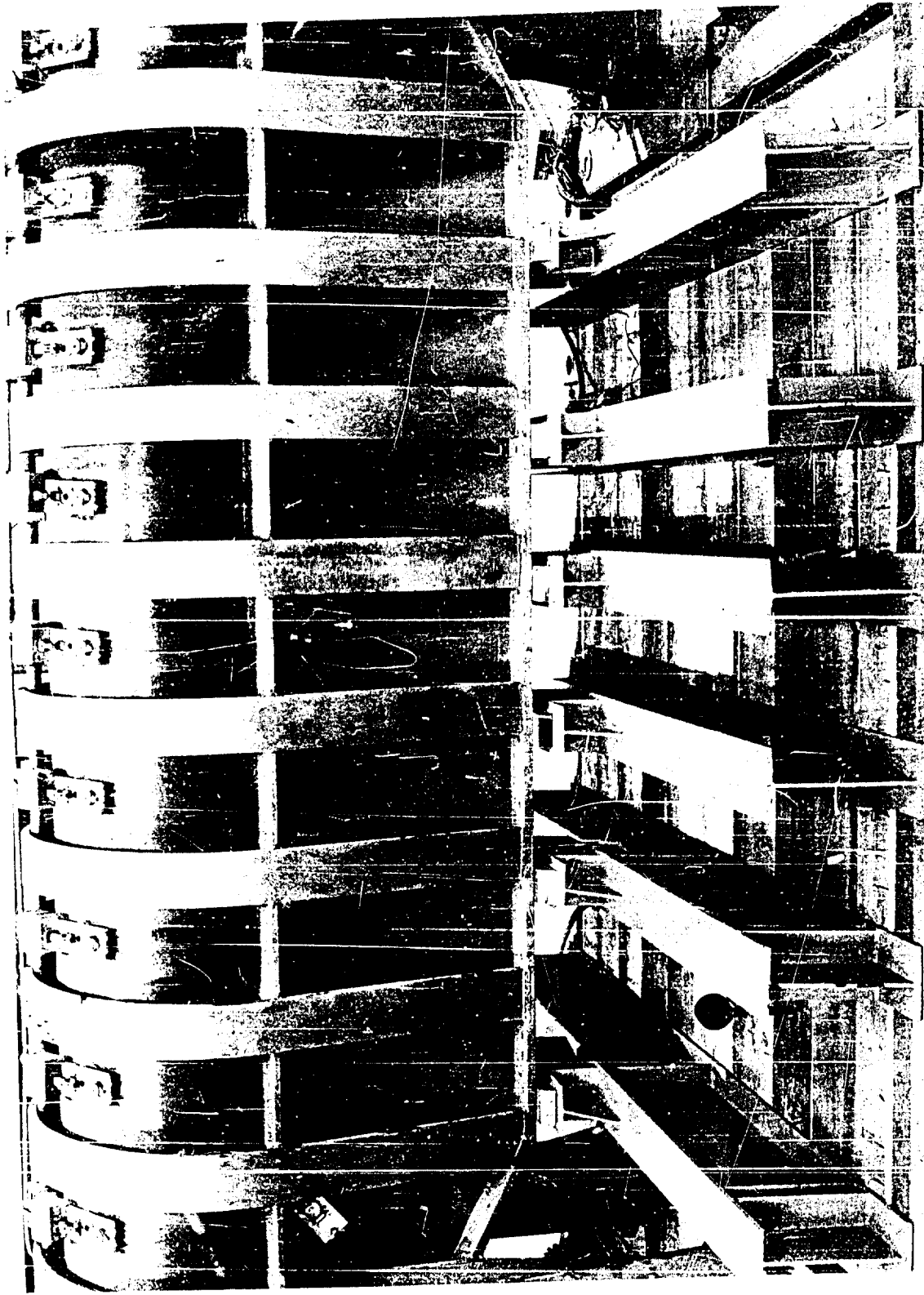


Figure 2. Reaction frame for static tests.

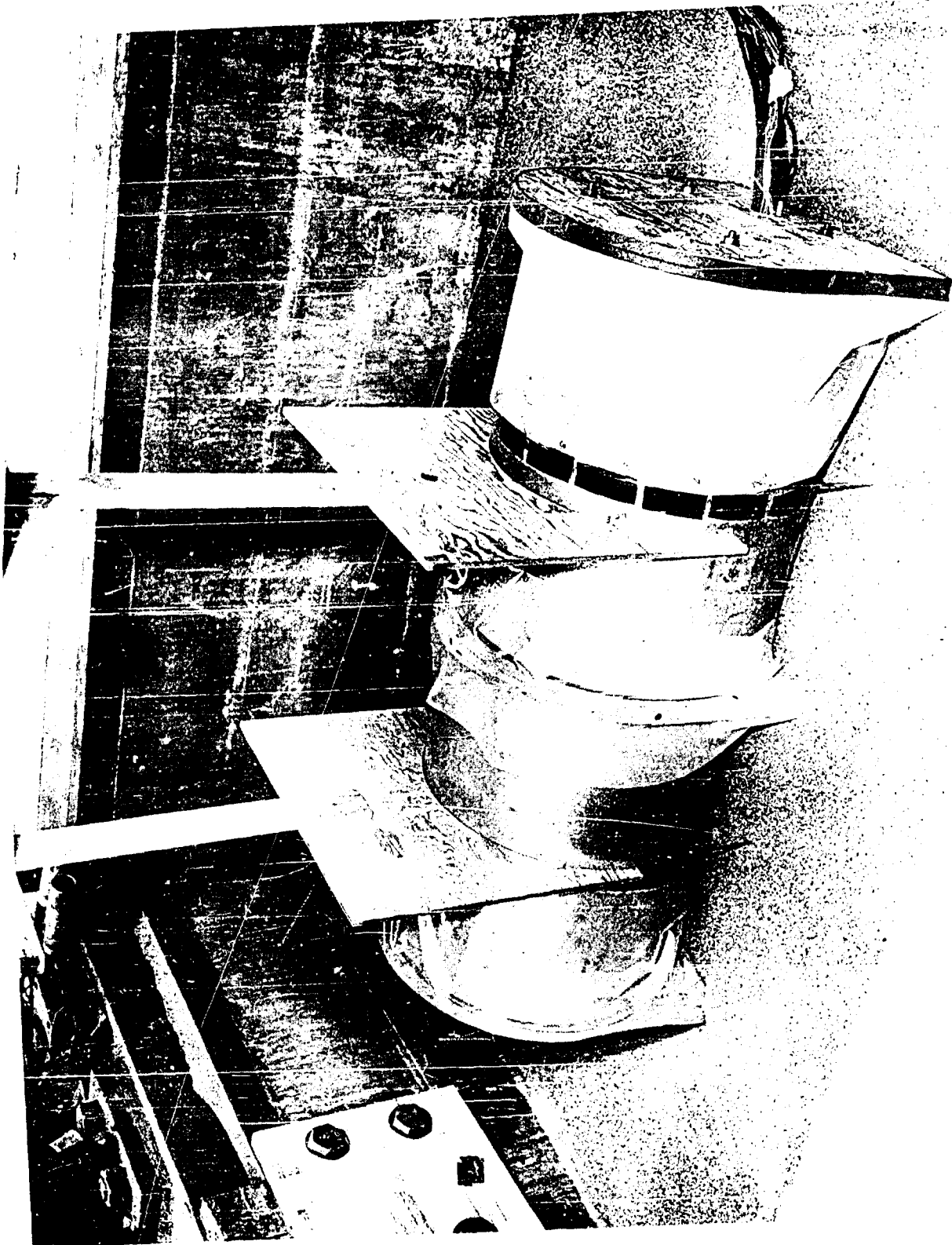


Figure 3. Small cylinders in test pit.

Table 1. Physical Properties of Cylinders

Material	steel
Modulus of Elasticity, E	$30 \times 10^6$ psi
Diameter, d	24 in.
Length	30 in.
Thickness	0.0478 in.
Weight (including instrumentation)	37 lb
Depth of crown below surface	9 in.
Natural period (covered, 1st inextensional mode)	21 msec
Moment of inertia, I (per inch of length)	$9.1 \times 10^{-6}$ in. <sup>4</sup>
Radius of gyration (per inch of length)	$1.38 \times 10^{-2}$ in.

As may be seen in Figure 3, plastic film 6 mils thick, held in place with cloth tape, kept sand from lodging between the edges of the cylinder and the end walls. Figure 3 also shows the plywood braces that held the cylinders firmly in place and retained the circular geometry during the backfill operation. Backfill was continued until the depth of cover over the crown was 9 inches, after which the backfill supports were removed. A 1-inch-thick layer of polyethylene foam was introduced around the top half of the circumference on a 16-inch radius of the left cylinder in Figure 3. The foam had a density of 35 pounds per cubic foot and compressive stress-strain characteristics as shown in Figure 4. The isolation material is not shown in the schematic instrumentation layout of Figure 6.

#### Instrumentation

Recording Equipment. Instrumentation was provided to measure pressures, strains, deflections, and accelerations. All measurements were recorded using Consolidated Electrodynamics Corporation (CEC) System D equipment with CEC 5-119 oscillographs. This is the same equipment used in previous similar dynamic tests of small buried arches.

Gas Pressure. During the static tests, pressure in the neoprene bag was measured with a Wallace and Tiernan Model FA-145 static-pressure gage; a Statham Model PA-208 TC pressure cell, calibrated against the Wallace and Tiernan gage, was mounted at the inlet to the bag.

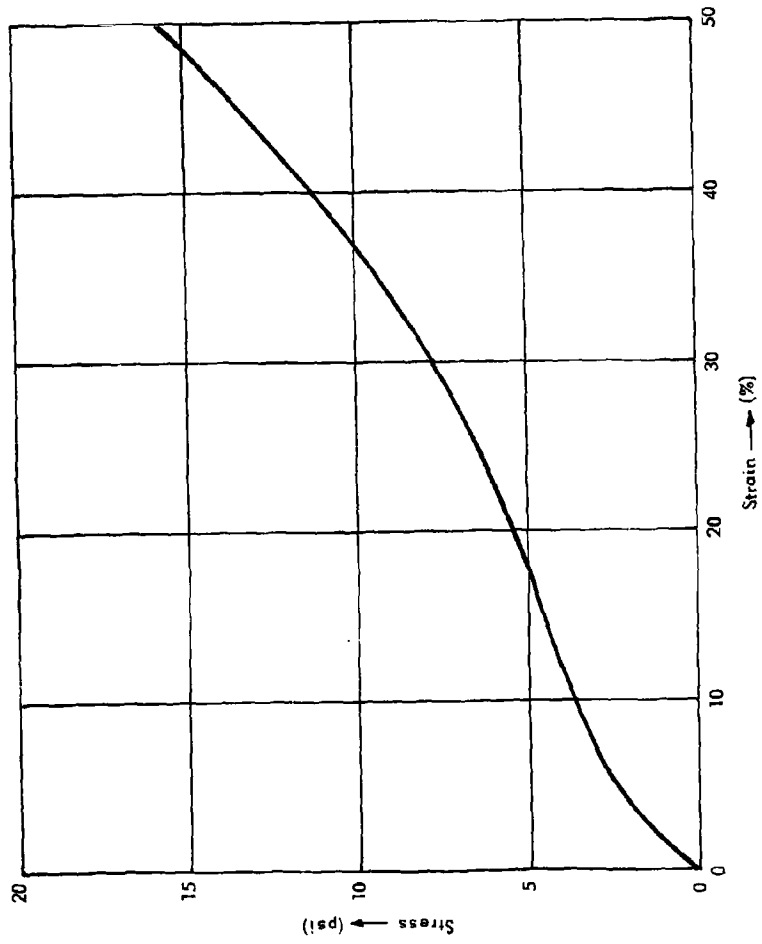


Figure 4. Stress-strain curve of polyethylene foam.

To measure the gas pressure during the dynamic tests, three Statham Model PA-208 TC pressure cells were mounted in the enclosure formed by the skirt extensions of the blast simulator. Two of these cells were placed on the surface of the sand near the center of the test pit, one with the face parallel and the other perpendicular to the direction of blast propagation. These gages measured the "face-on" and "side-on" pressures. A third pressure cell was mounted in one of the skirt extensions about midway between the simulator and the surface. These pressure cells also were calibrated with the Wallace and Tiernan Model FA-145 static-pressure gage prior to installation.

Due to a combination of lateral acceleration (to which these pressure cells are highly susceptible) and the reflected pressures in the enclosure, the reading of the "face-on" gage turned out to be the only reliable pressure measurement obtained during the dynamic tests.

Strains. Strains in the cylinders were measured with SR-4 bonded strain gages, Type A-1, with a gage factor of 1.98. These gages were placed at the locations shown in Figures 5 and 6. This particular spacing of gages was used to enable the determination of thrust and moment distributions with a minimum number of channels of instrumentation.

Deflections. Two types of deflection measurements were made: "internal" and "external." Measurements to determine the movement of the cylinders relative to the foundation of the simulator are called "external," while measurements of the change in dimensions of the cylinder are called "internal." The external measurements were made with Bourns linear-motion potentiometers, Model 108, with a maximum travel range of 1.1 inches. Model 156 Bourns potentiometers were used for the internal measurements. These gages were capable of 4 inches of travel, with the exception of potentiometer number D4-S which allowed only 2.5 inches of travel. All potentiometers were calibrated versus an ordinary linear scale.

Interface Pressures. Both CEC 4-312A and Statham Model PA-208 TC pressure pickups were used to detect interface pressure. These transducers were mounted in a hole cut through the arch so that their faces were flush with the extrados. They were covered with a thin plastic film prior to placement of the backfill. It was realized that the magnitudes indicated by these gages may not be realistic; however, it was expected that the time-phase information would be accurate and useful. The interface-pressure gages were calibrated with the previously mentioned Wallace and Tiernan static gage.

Accelerations. Statham Model A52 accelerometers with a 100-g range were attached to the bottom of the cylinders at the 180-degree point as shown in Figures 5 and 6. These transducers were calibrated with a centrifuge-type accelerometer calibrator.

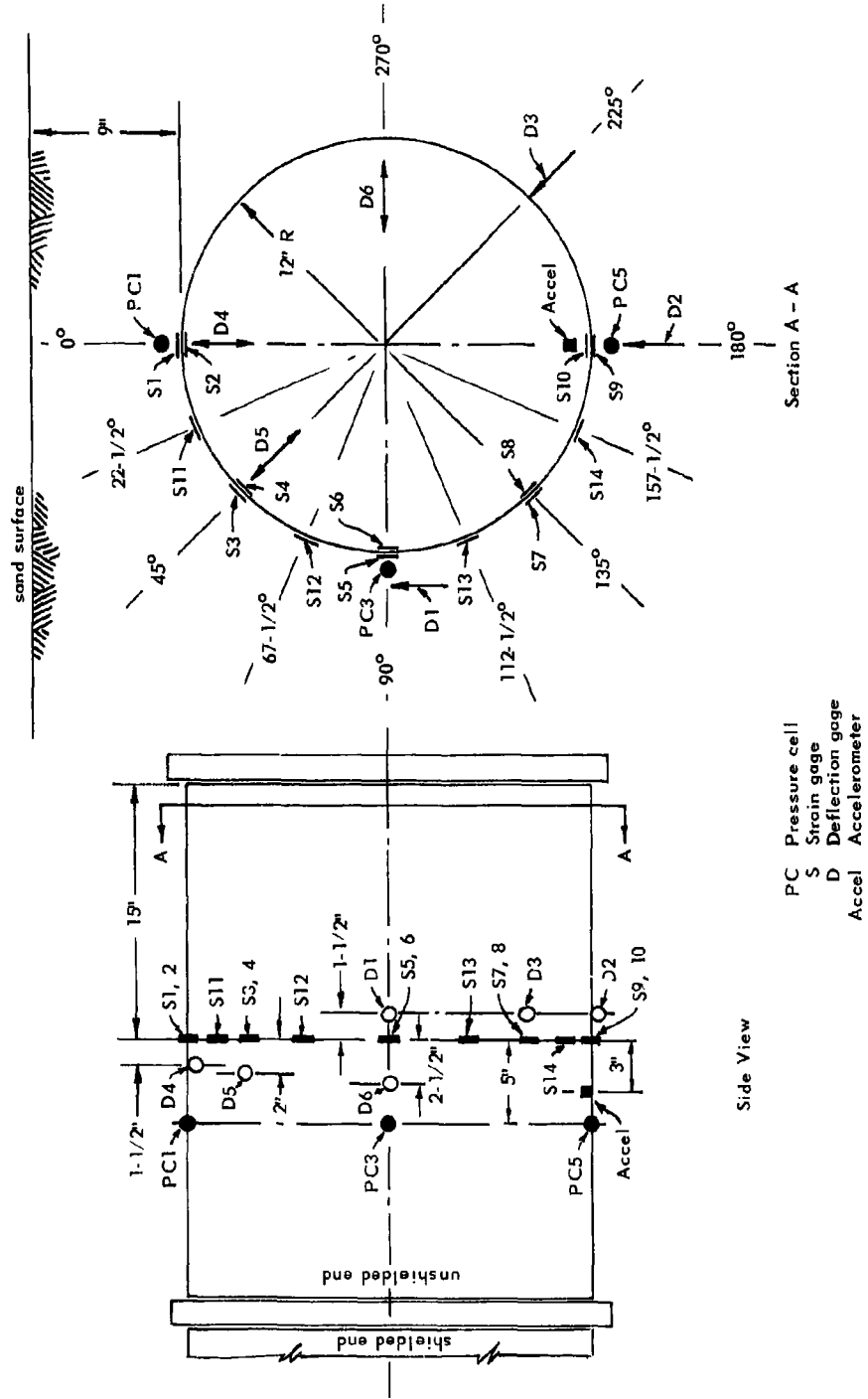


Figure 5. Instrumentation layout — Unshielded cylinder.

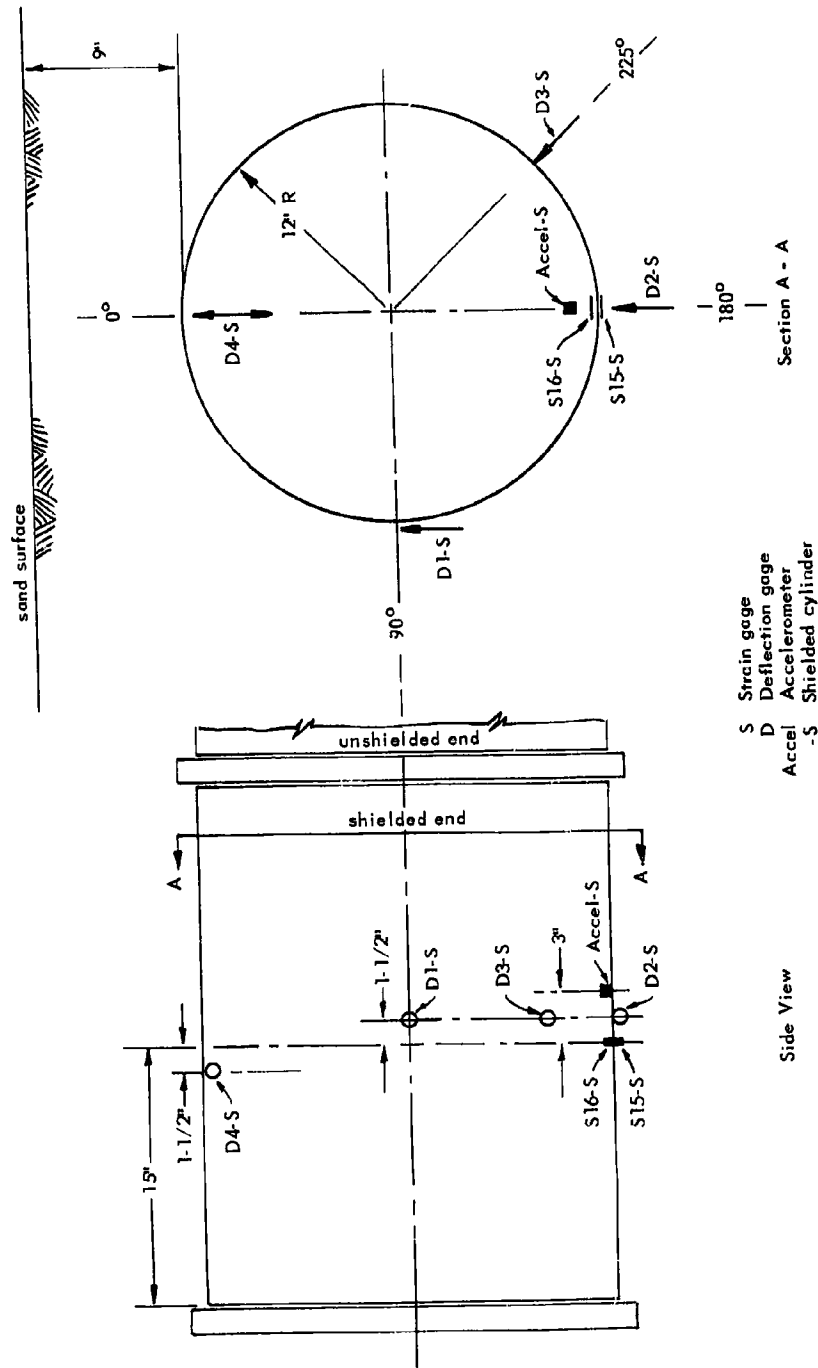


Figure 6. Instrumentation layout — Shielded cylinder.

Measurement Errors. Except for soil pressures, the maximum error likely from any of the measurements is  $\pm 7$  percent. The accuracy of the soil-pressure measurements remains unknown.

#### Test Program and Procedure

Four different types of tests were performed on the soil-cylinder system: vibration tests, backfill tests, and static and dynamic load tests. The static and dynamic tests employed two completely different setups; the vibration tests and backfill tests were performed in conjunction with the static and dynamic tests in the order delineated below.

Vibration Test — Cylinders Uncovered. Prior to placing the cylinders in the test pit for the static experiments, one of them was vibrated to determine its first inextensional symmetrical mode of vibration. To do this, the cylinder was supported upon a flat surface and struck a moderately sharp blow with the hand at the top, or zero-degree, point. The ensuing vibration was recorded as registered by the strain gages, internal deflection gages, and accelerometer.

Backfill Test — Static Loadings. Following the uncovered vibration test, the cylinders were installed in the pit on the sand that had previously been placed to the proper elevation. They were then blocked in place as shown in Figure 3, and an oscillograph record was taken to establish the "zero" for all measurements. Thereafter, the backfill was carefully placed and compacted as described in Appendix A. When the backfilling and final compaction were completed, the backfill supports were removed and a second record was taken to permit determination of the induced deflections, thrusts, moments, and interface pressures.

Static Tests. Upon completion of placement of the reaction system shown in Figure 2, the soil-structure system was loaded twice to 10 psi and twice to 25 psi. In Tests 1 and 2, records were taken in increments of 1 psi on loading to 10 psi, and at 7 psi, 3 psi, and 0 psi on unloading. In Tests 3 and 4, the system was loaded to 25 psi in two cycles, with records taken at each 2-psi increment and at 25 psi during loading and in increments of 5 psi while unloading. The rate of loading was approximately 2 psi per minute in all tests.

Before each test, all instruments were rebalanced so as to record only the response due to that particular loading. During the sequence of static loadings, the soil was not disturbed in any manner.

Backfill Test — Dynamic Loadings. After completion of the static tests, the structure was relocated in the test pit and the soil was replaced and compacted, following the same procedure as for the static tests. The test procedure was identical to that used in the backfill test for the static loadings.

Vibration Pretest — Cylinders Covered. The buried cylinders were vibrated by detonating a 0.01-pound charge of composition C4 high explosive 1 foot above the sand surface. The charge was not large enough to disturb the soil backfill or otherwise materially alter the system. Records were taken of the response of all instruments to enable determination of the natural period. During this and all subsequent tests, the surface of the sand was covered with a 6-mil plastic film to prevent gas pressure from entering the voids in the sand.

Dynamic Tests. After completion of the vibration test, four long-duration dynamic loadings were applied to the surface of the soil-structure system. A loading sequence was followed as for the static tests to determine the effect of repeated loading. The first two tests were intended to be 10-psi shots, and the final two were intended to be 25-psi shots. Actual pressures varied somewhat from the programmed pressures as will be subsequently observed. The reason for this is probably due to the variation in heat loss to the simulator when operating at low overpressures with the correspondingly small charges. This does not markedly affect the test results since the actual pressures obtained are known.

As in the static tests, the soil was not disturbed in any way between tests, and all instrumentation was rebalanced before each loading.

Vibration Post-Test — Cylinders Covered. A vibration test was performed after completion of the dynamic tests to determine if any appreciable change in the natural period of the structure had occurred due to possible changes in the soil conditions. The procedure followed was identical to that employed during the vibration pretest.

## RESULTS AND DISCUSSION

### Introduction

Results are presented and discussed in this section in essentially the same order as the experiments were performed as described in the preceding section. The tests were performed with essentially no difficulties, due largely to experience gained in previous similar model arch tests. The full significance of the experiments is more nearly realized when interpreted in the light of information gained from

theoretical and other experimental work — as attempted in the companion report, TR-344.<sup>2</sup> The discussion which follows is restricted almost entirely to results from the described test program.

### Natural Period

When the cylinder was placed on a flat surface and struck with a sharp blow on the top, it was found to vibrate in the first inextensional mode with a period of 200 milliseconds. On a few of the gage traces there appeared to be a superimposed vibration with a period of 52 milliseconds. After the structure had been placed in the test pit and covered, it was found that the unshielded cylinder would not vibrate sufficiently under excitation from detonation of a 0.01-pound charge to permit determination of the fundamental natural period. A larger charge was not employed because of the danger of seriously disturbing the system. The motion damped out almost completely in one cycle. The upper portion of the shielded cylinder, however, did vibrate at a natural period of 23 milliseconds.

### Backfill Tests

It was recognized that the response of a buried flexible cylinder to surface loading could be influenced considerably by distortions introduced during backfilling. Therefore, care was taken during this test program to minimize these distortions, the magnitudes of which were measured during the backfill tests. Procedures and results of the backfill tests prior to the static and dynamic surface loadings were sufficiently similar that only the results of the backfill test preceding the dynamic tests are presented and discussed in this section.

As described earlier in this report and shown in Figure 3, supports were placed on the cylinders to hold them in a circular configuration during placement of the surrounding soil. Zero records were taken with the cylinders in this position. Data from records taken after backfilling was completed are given in Table II, from which it can be seen that deflection of the cylinders consisted of a flattening in the vertical plane with considerable upward movement of the crown and only slight downward movement of the base. The interface pressure data show that this deflection was caused by comparatively high soil stresses at the sides of the cylinders.

Under the conditions of testing, thrust and moment data had little meaning; thus, these data are not presented in Table II. Before zero readings were taken, compressive stresses were set up in the cylinders by the backfill supports. Therefore, the final strain readings noted only the difference between the compressive strains caused by the supports and the strains (predominantly compressive) present after completion of backfilling and removal of the supports. Clearly, the final strains

could be greatly influenced by the type and effectiveness of the supports used. Consequently, these backfill experiments were basically an evaluation of the effectiveness of the backfill supports rather than an evaluation of cylinder response to backfilling.

Table II. Backfill Test Data

Gage	Deflection (in.)	Gage	Pressure (psi)
D1	-0.204	PC-1	0.76
D2	0.011	PC-2	2.14
D3	-0.039	PC-3	0
D4	-0.220		
D5	0.191		
D6	0.175		
D1-S	-0.122		
D2-S	0.023		
D3-S	-0.035		
D4-S	-0.163		

+ deflection = downward or increase in length of diameter

+ pressure = greater than atmospheric

### Static Tests

Deflections of the shielded and unshielded cylinders resulting from static surface loadings are presented in Table III and in Figures 7 and 8. The nature of these deflections may be better appreciated by referring to Figure 9, which shows the components of deformation due to a uniform surface loading. As shown, deflection of a thin-walled buried cylinder subjected to a uniform surface loading is characterized by (1) body motion of the structure with and into the soil, (2) flattening in the vertical direction, (3) reduction of the perimeter due to compression, and (4) development of circumferential waves. The component of body motion of prime concern is the vertical deflection of the undeformed cylinder with respect to a point in the free field at the elevation of the original horizontal centerline. This deformation is the distance  $y_b$  in Figure 9a; distance  $a-a'$  in this figure represents deflection of the free-field soil. Relative body motion depends largely upon characteristics of the bedding beneath the cylinder and is exceedingly important since such motion, and the compressive deformation, govern the amount of arching that develops in the soil bridge over the cylinder.



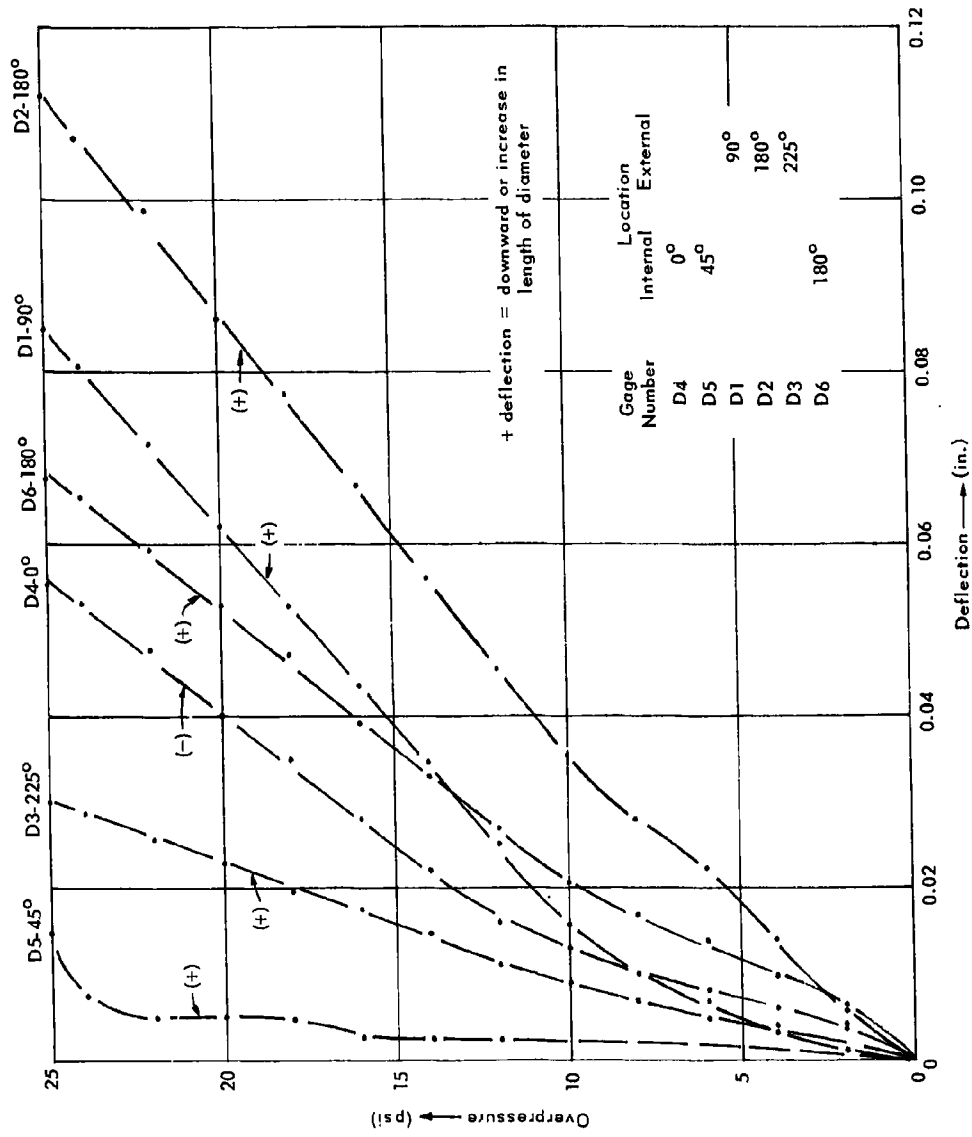


Figure 7. Overpressure vs deflection — Unshielded cylinder.

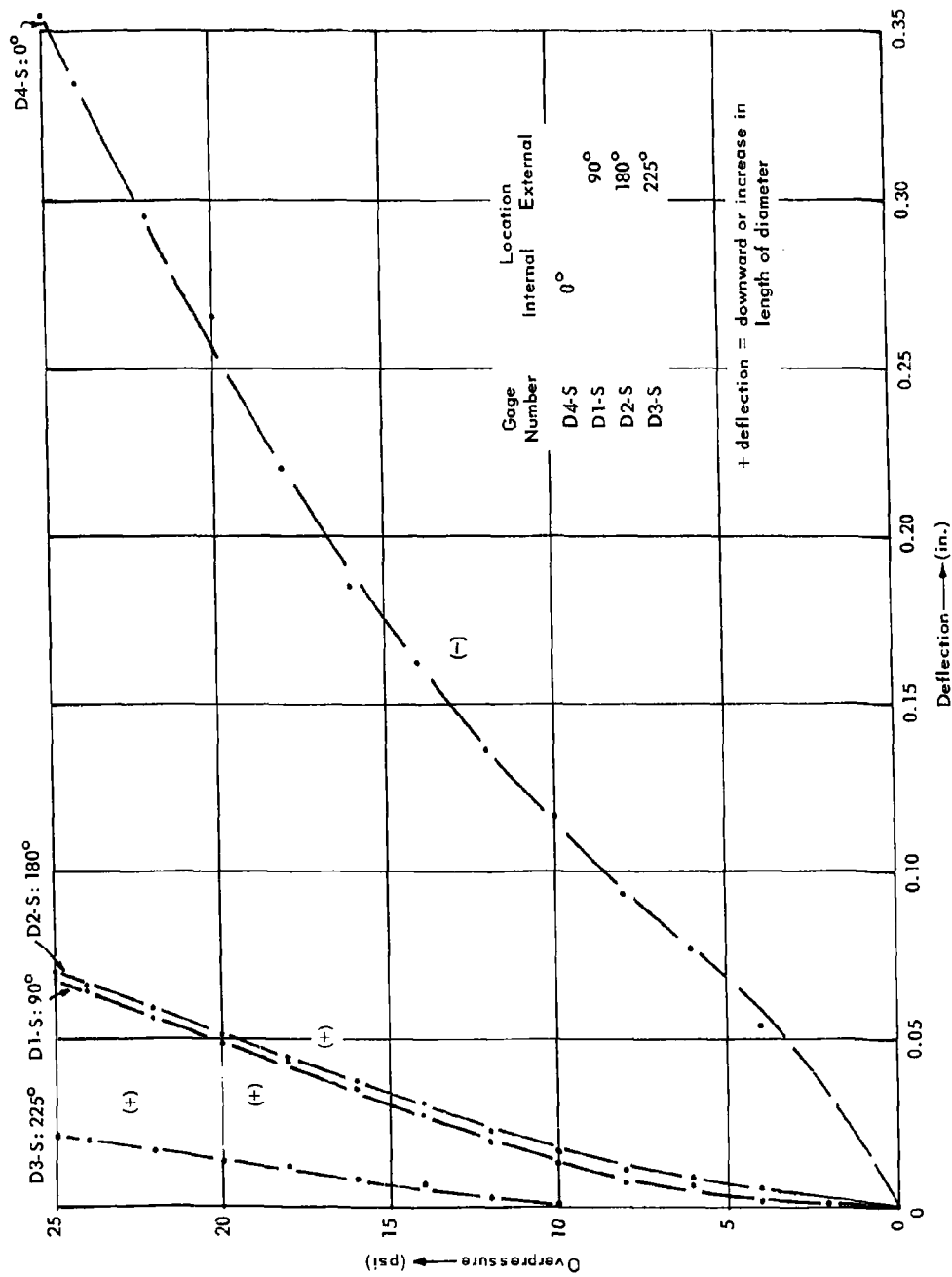


Figure 8. Overpressure vs deflection — Shielded cylinder.

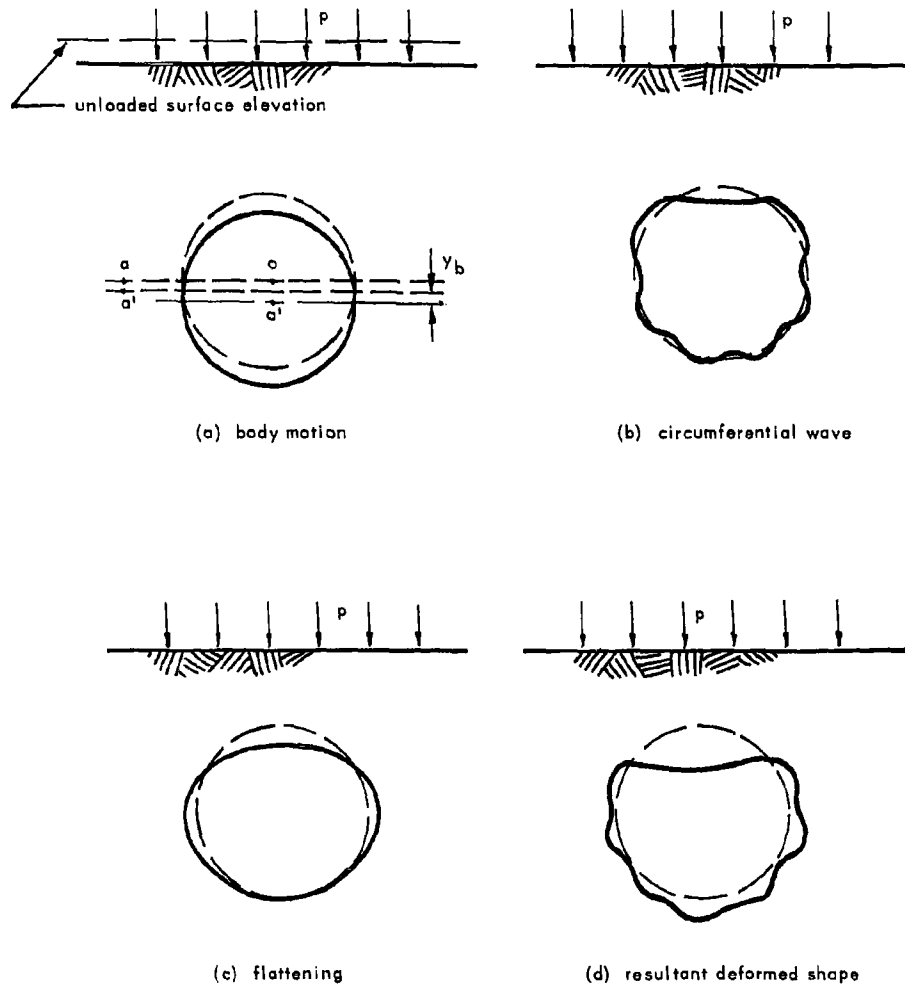


Figure 9. Deflections of shallow-buried cylinder.

Radial compressive deformation is usually negligible in metal cylinders. By contrast, the flattening, or first-mode deformation, indicated in Figure 9c, is usually appreciable. Flattening is due to the difference in compliance of the soil and the cylinder, the anisotropic properties of soil, and the presence of the surface boundary. When an increment of load,  $\Delta p$ , is applied to the soil surface, the vertical soil stress on the cylinder, assuming no arching, will also be  $\Delta p$ , but the horizontal load on the cylinder will only be  $K_0(\Delta p)$ , where  $K_0$  is the coefficient of lateral earth pressure at rest. Obviously, the cylinder is not in equilibrium under these conditions; consequently, it tends to flatten and in the process to develop lateral earth pressures that result in a very nearly uniform radial pressure around the cylinder as the system achieves equilibrium. This process is continued on the application of each successive load increment, with the soil and the structure always interacting in such a way as to achieve a nearly uniform radial distribution on the cylinder, which it is ideally suited to resist. This action is evidenced in the interface pressure data of Table IV where it may be noted that the interface pressure at the 45- and 90-degree stations is in most cases within a few percent of the surface overpressure. In all probability, the gage at the crown reads less than the surface pressure because of active arching across the gage; likewise, the gage at the 45-degree station reads more than the surface pressure because of passive arching. Apparently, at 90 degrees the increase in surface pressure due to passive arching was offset by the difference between horizontal and vertical pressures at a point in the soil, with the result that the pressure at 90 degrees was less than the surface pressure. Difficulty in controlled placement of the soil in the vicinity of the gage faces is probably responsible for the unreasonable readings of the two lower gages. As previously mentioned, soil pressures are the least reliable of all measurements taken.

It has been shown<sup>6</sup> that, in the process of deforming, circumferential waves develop around the perimeter as indicated in Figure 9b. The number of waves which develop are dependent on the ratios of thickness to radius and length to radius, and are influenced by the stiffness of the soil and the surface boundary.<sup>2</sup> The presence of the surface boundary causes the upper portion of a shallow-buried cylinder to deform in the shape of a simply supported arch. The resultant deformed shape, exaggerated for illustration purposes, and accounting for all components of the deformation, is shown in Figure 9d. Understanding the basic modes of deformation materially aids in comprehending the significance of the other test data.

Two particularly interesting observations may be made from the deflection data of Table III: (1) the deflections of the crown of the shielded cylinder were considerably larger than for its unshielded counterpart; and (2) conversely, the downward deflection of the bottom of the shielded cylinder was slightly less than the downward deflection of the bottom of the unshielded cylinder. Further, the

body motion of the shielded cylinder was slightly less than for the unshielded cylinder. It may be noted from Figure 7 that for pressures greater than 10 psi, overpressure versus deflection plotted as a straight line for all points on the unshielded cylinder except the 45-degree point.

The resulting deformed shape of the unshielded cylinder as measured by the potentiometers is indicated in Figure 10. The circumferential waves could not be distinguished in the deflection measurements; however, the wave shape can be inferred from the moment diagram, Figure 11.

Values of the moments and thrusts computed from the strain data in Table V are given in Table VI and are shown pictorially in Figures 11 and 12. From Figure 11 it may be observed that the maximum moment at the bottom of the cylinder had a magnitude several times the moment at the crown or elsewhere around the cylinder. The period of the circumferential waves at the bottom and at the side is approximately 50 degrees; however, the wave shape is materially altered near the top of the cylinder due to the presence of the surface boundary. Computation of moments at the 22.5-degree points (22.5°, 67.5°, 112.5°, and 157.5°) was accomplished by interpolating the thrust values at these points from Figure 12 and, with the knowledge of the strain at the extrados, computing the strain on the intrados corresponding to the interpolated thrust. This procedure was fairly reliable because of the uniformity of the thrust distribution around the cylinder.

The distribution of thrust around the perimeter is essentially uniform and equal to the product of the surface pressure and the radius of the cylinder — except near the top and bottom of the cylinder, where the thrust decreases. The fact that the thrust at the 90-degree point is almost exactly equal to the product of the surface pressure times the radius of the cylinder leads to the conclusion that the net arching across the cylinder was very nearly zero.

It should be noted that when strains at the intrados and extrados of the cylinder at a point are of nearly the same absolute magnitude and the operation involved in computation of either thrust or moment is subtraction of these absolute values, errors of a large percentage can occur in the computed thrusts or moments at that point.

The preceding discussion has dealt almost entirely with the results of the first loading to 25 psi. Upon removal of the load, the cylinder rebounded somewhat from its deformed position, but a portion of its deformation was residual. In all cases, the deflections resulting from the second loading to 25 psi were less than those from the first loading; however, the cumulative deformations were slightly greater.

Table IV. Interface Pressure Distribution Due to Static Loading

Overpressure (psi)	0° PC1 (psi)	45° PC2 (psi)	90° PC3 (psi)	135° PC4 (psi)	180° PC5 (psi)
2	1.8	2.8	2.3	1.4	-0.01
4	3.5	5.4	4.1	2.7	-0.01
6	5.1	7.7	5.9	4.0	-0.01
8	6.2	9.5	7.5	5.0	-0.02
10	7.7	11.7	9.2	6.2	-0.03
12	9.3	14.0	11.0	7.4	-0.03
14	11.0	16.3	12.7	8.3	-0.01
16	12.4	18.4	14.4	9.2	0
18	13.9	20.7	16.1	10.2	0.05
20	14.8	22.7	17.7	11.1	0.14
22	15.9	24.8	19.5	12.1	0.25
24	17.1	26.7	21.1	13.0	0.55
25	17.6	27.7	21.9	13.7	0.75

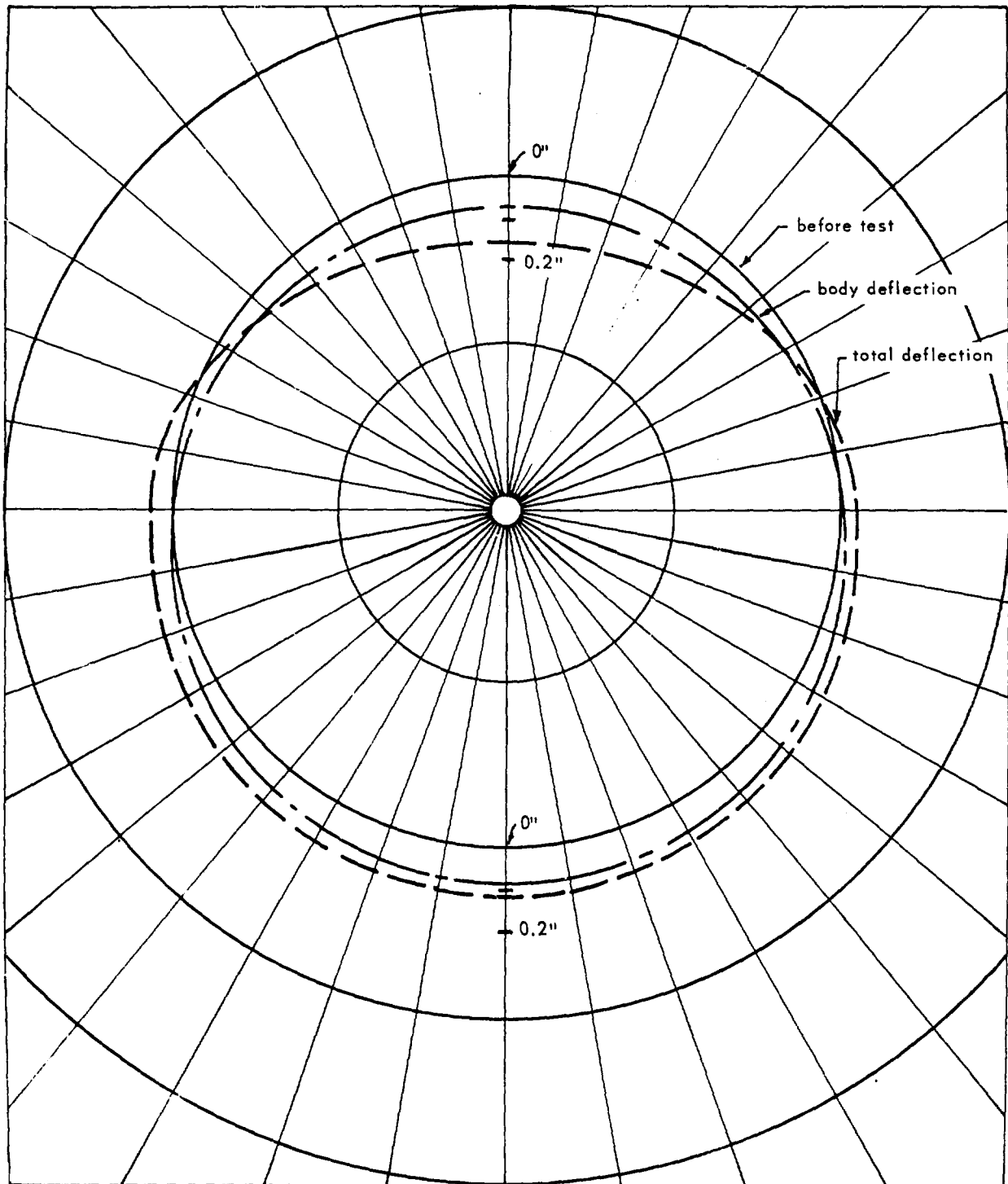


Figure 10. Peak cylinder deflection at 25 psi — Static test of unshielded cylinder.

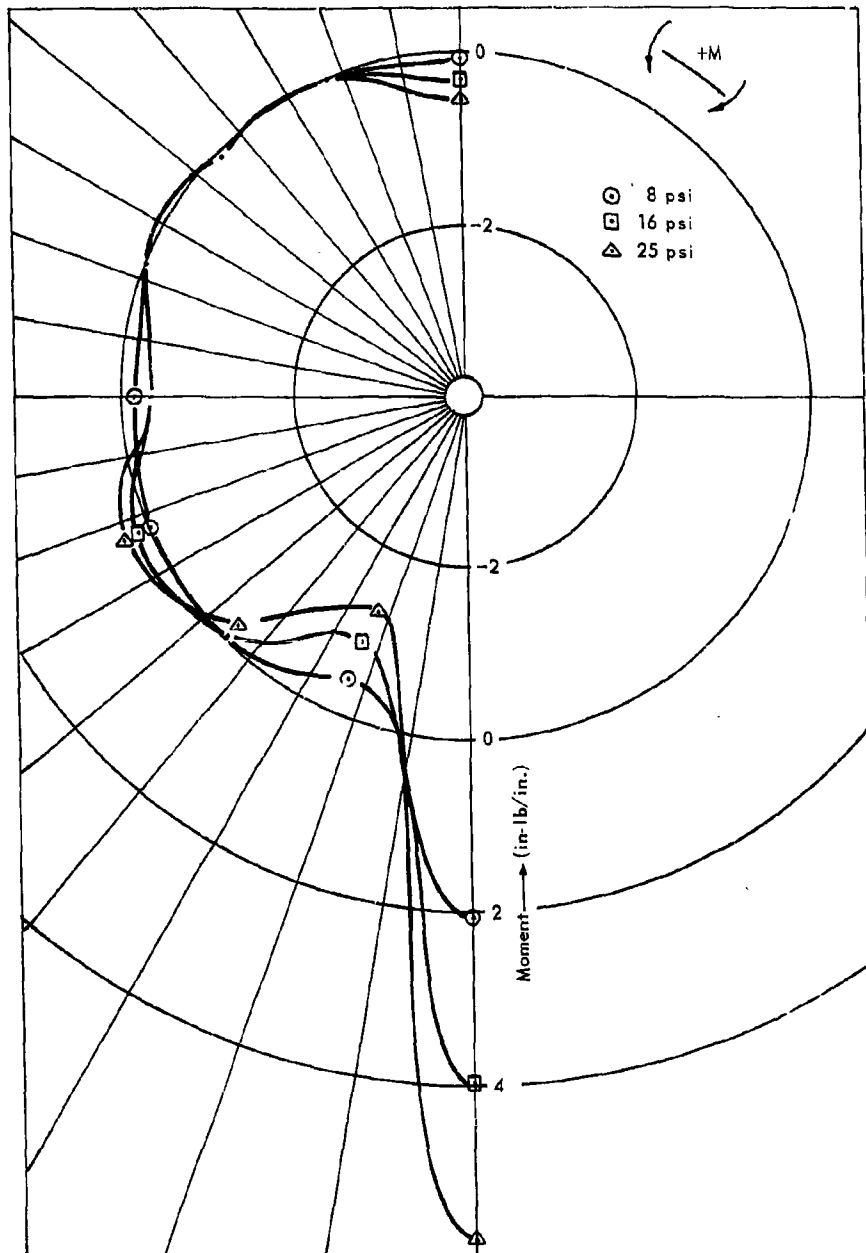


Figure 11. Moment diagram — Static test of unshielded cylinder.

Table V. Strains due to Static Loading

Surface Pressure (psi)	Strain ( $\mu$ in./in.)															
	S1	S2	S3	S4	S5	S6	S7	S8	S9	S10	S11	S12	S13	S14	S15-S	S16-S
Test No. 1																
1	-2	-6	-8	-12	-9	-6	-2	-4	12	-12	-6	-5	-2	-4	2	-2
2	-16	-10	-13	-20	-18	-12	1	-10	41	-46	-13	-11	-5	-15	10	-13
3	-26	-15	-21	-32	-26	-15	-2	-20	75	-86	-21	-17	-9	-29	19	-28
4	-36	-19	-27	-41	-38	-18	-5	-30	108	-127	-31	-24	-12	-42	31	-45
5	-48	-24	-34	-49	-44	-24	-7	-37	142	-164	-37	-31	-16	-52	43	-62
6	-58	-27	-42	-59	-56	-30	-12	-46	173	-205	-45	-37	-21	-62	53	-78
7	-69	-33	-51	-69	-64	-38	-17	-55	205	-244	-55	-45	-24	-70	64	-92
8	-79	-37	-59	-79	-73	-44	-23	-63	232	-273	-61	-52	-28	-78	74	-110
9	-89	-41	-66	-87	-82	-50	-30	-71	262	-308	-68	-59	-32	-84	83	-123
10	-101	-44	-74	-96	-91	-56	-36	-77	287	-336	-75	-65	-35	-91	93	-138
7	-75	-24	-45	-69	-62	-27	-16	-57	293	-326	-52	-30	-19	-81	97	-132
3	-42	-6	-9	-33	-26	-3	9	-37	234	-254	-27	4	-2	-70	79	-103
0	-8	-24	9	2	9	9	24	-14	104	-94	-	23	5	-55	41	-42
Test No. 2																
1	-10	-3	-6	-11	-12	-2	-2	-7	4	-2	-8	-7	-5	-6	-1	2
2	-19	-9	-14	-22	-32	-6	-4	-14	30	-33	-17	-14	-9	-11	6	-9
3	-29	-15	-21	-32	-31	-11	-9	-21	56	-63	-24	-22	-13	-17	12	-18
4	-38	-21	-28	-41	-43	-17	-13	-27	81	-90	-30	-29	-18	-22	18	-28
5	-46	-27	-35	-50	-52	-22	-17	-32	105	-115	-37	-36	-22	-27	24	-37
6	-54	-33	-44	-60	-61	-29	-26	-37	125	-141	-44	-44	-26	-31	31	-47
7	-61	-39	-51	-69	-69	-35	-29	-43	143	-164	-51	-53	-31	-35	38	-56
8	-70	-45	-59	-77	-77	-40	-34	-48	167	-187	-56	-59	-35	-41	44	-67
9	-77	-51	-66	-86	-85	-47	-40	-55	188	-213	-64	-57	-39	-45	50	-79
10	-87	-56	-75	-94	-93	-54	-47	-61	210	-238	-69	-75	-43	-50	60	-91
7	-67	-34	-49	-70	-66	-28	-31	-46	208	-234	-52	-47	-27	-38	61	-89
3	-34	-7	-12	-33	-29	1	-5	-27	155	-162	-25	-11	-9	-24	45	-57
0	-	9	6	2	-34	5	8	-3	20	-10	2	9	-1	-7	7	-

- strain tension

Test No. 3																
2	-20	-5	-16	-21	-24	-6	-4	-16	30	-35	-17	-15	-8	-11	4	-10
4	-36	-20	-30	-38	-43	-16	-12	-28	80	-96	-42	-31	-18	-23	18	-32
6	-54	-32	-45	-59	-61	-31	-32	-40	125	-146	-45	-46	-26	-32	32	-49
8	-70	-44	-61	-77	-79	-45	-36	-52	160	-197	-59	-64	-36	-41	44	-71
10	-88	-58	-77	-94	-96	-59	-48	-62	200	-242	-72	-79	-44	-49	58	-93
12	-108	-72	-96	-112	-114	-75	-57	-75	240	-292	-87	-98	-52	-60	75	-120
14	-128	-82	-112	-130	-132	-92	-87	-87	275	-343	-101	-113	-63	-71	95	-148
16	-148	-94	-140	-145	-148	-104	-105	-97	315	-383	-114	-128	-71	-83	113	-177
18	-166	-106	-150	-165	-165	-122	-125	-109	345	-429	-138	-146	-79	-92	130	-203
20	-184	-116	-167	-183	-183	-138	-147	-121	375	-474	-142	-165	-89	-103	147	-228
22	-204	-124	-183	-198	-199	-155	-167	-129	410	-509	-154	-180	-99	-114	165	-254
24	-220	-134	-201	-215	-216	-171	-190	-141	435	-550	-166	-201	-109	-126	179	-277
25	-230	-140	-213	-224	-228	-183	-206	-151	435	-580	-175	-217	-115	-131	188	-289
20	-200	-108	-169	-186	-185	-136	-180	-123	450	-565	-145	-165	-87	-111	190	-285
15	-164	-76	-124	-148	-142	-92	-147	-97	440	-555	-114	-119	-59	-88	188	-281
10	-126	-40	-77	-106	-98	-47	-107	-69	410	-504	-81	-67	-28	-58	171	-244
5	-84	-4	-32	-65	-53	-10	-55	-46	320	-383	-48	-21	-4	-32	133	-185
0	-22	22	-4	-3	-6	-4	8	-12	50	50	-1	15	4	-15	34	-35

Test No. 4																
2	-26	-8	-16	-24	-30	-6	-8	-18	25	-40	-20	-18	-8	-13	4	-4
4	-44	-18	-30	-44	-53	-14	-20	-28	85	-106	-34	-33	-16	-23	22	-28
6	-60	-28	-45	-62	-73	-26	-35	-38	135	-166	-49	-48	-28	-34	34	-50
8	-78	-40	-61	-77	-91	-40	-53	-50	175	-217	-63	-67	-38	-41	46	-71
10	-94	-52	-77	-94	-110	-55	-69	-60	205	-257	-75	-82	-48	-53	58	-91
12	-112	-66	-94	-115	-130	-73	-87	-73	235	-303	-89	-103	-61	-64	71	-111
14	-128	-78	-112	-130	-146	-87	-104	-83	260	-338	-101	-121	-71	-77	83	-133
16	-144	-90	-128	-148	-175	-105	-122	-97	285	-378	-115	-139	-81	-84	97	-153
18	-162	-104	-148	-168	-185	-123	-140	-111	305	-413	-129	-160	-93	-96	111	-175
20	-180	-116	-165	-183	-201	-139	-159	-121	330	-444	-142	-199	-103	-107	125	-196
22	-198	-130	-187	-204	-220	-155	-205	-137	340	-489	-157	-203	-113	-120	141	-222
24	-218	-144	-205	-221	-240	-178	-216	-151	355	-529	-171	-224	-125	-133	151	-244
25	-224	-148	-215	-230	-248	-186	-216	-155	365	-540	-176	-230	-131	-141	159	-260
20	-192	-116	-171	-189	-205	-139	-187	-127	375	-524	-147	-179	-101	-118	165	-256
15	-156	-82	-124	-151	-159	-91	-155	-99	380	-509	-115	-133	-71	-94	163	-246
10	-116	-48	-77	-109	-112	-44	-114	-69	350	-464	-82	-82	-40	-66	141	-212
5	-74	-10	-26	-62	-65	-4	-55	-42	280	-348	-46	-30	-14	-38	135	-155
0	-14	14	-8	-3	-2	-	4	-8	25	-30	1	6	-2	-11	14	-6

Table VI. Moments and Thrusts Due to Static Loading  $\perp$

Over- pressure (psi)	0°		45°		90°		135°		180°		Shielded End 180°	
	Moment	Thrust	Moment	Thrust								
8	-0.15	-82	0.09	-99	-0.19	-89	-0.09	-63	2.04	-26	0.65	-20
16	-0.31	-174	0.03	-204	-0.25	-180	-0.04	-145	3.99	-48	1.66	-46
25	-0.51	-265	0.07	-313	-0.26	-295	-0.31	-256	5.79	-104	2.73	-72

$\perp$  Moments = in-lb/in. Thrusts = lb/in.

+ moment creates tension in outside fibers of cylinder.

+ thrust = compression.

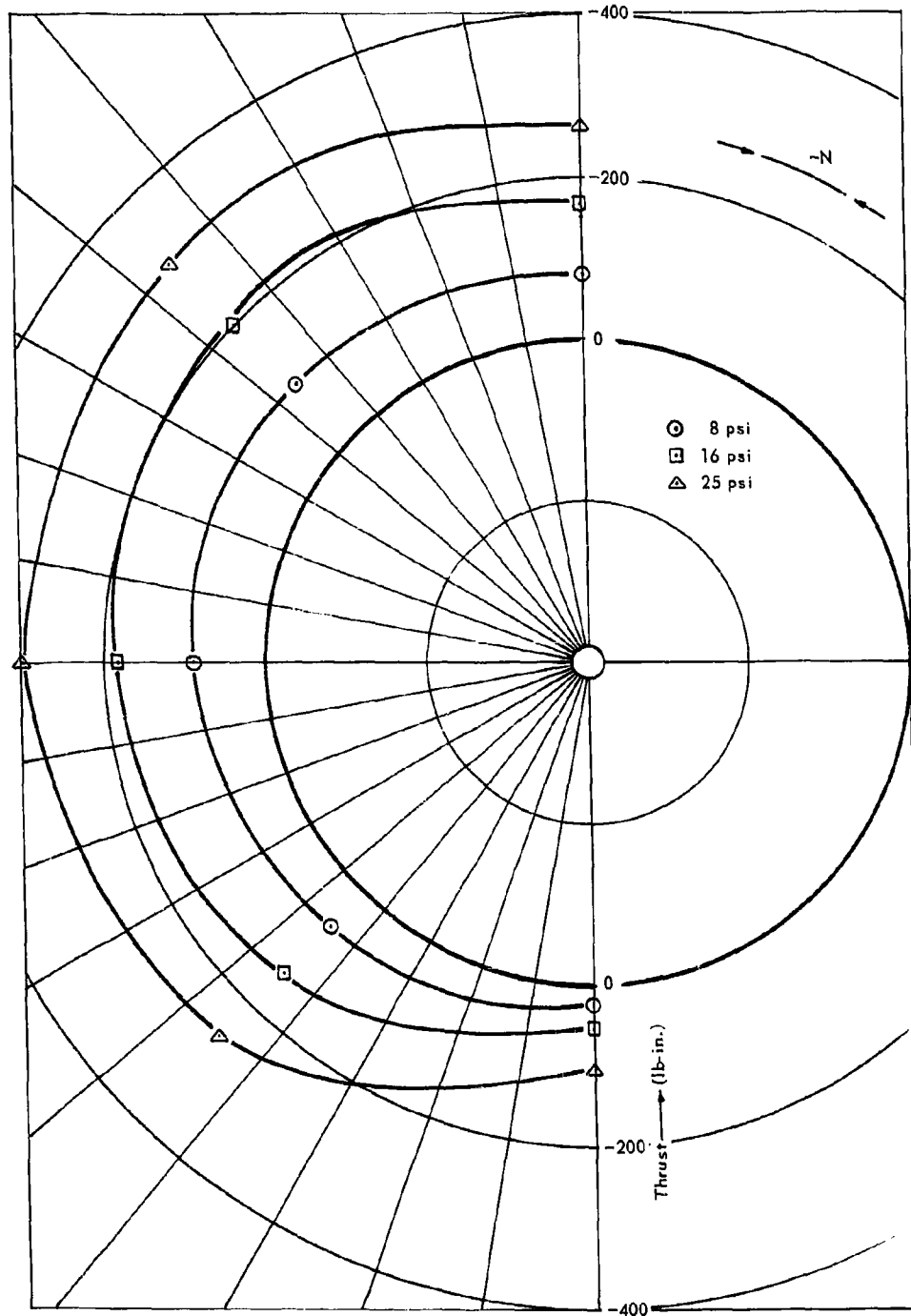


Figure 12. Thrust diagram — Static test of unshielded cylinder.

In the companion report, Reference 2, it is shown that relatively large deformations are required to develop active arching. A cylinder which does not experience slippage at the joints or plastic yielding is incapable of developing sufficient deformations to produce appreciable arching. If a designer chooses to take advantage of the arching in the soil, he must employ a soft bedding in the cylinder or use plating with slip joints.

#### Dynamic Tests

Data on the actual maximum applied pressures for the dynamic loading and the corresponding peak deflections are given in Table VII for the unshielded cylinder. The actual peak overpressures differed slightly from the programmed overpressures of 10 psi for Tests 1 and 2 and 25 psi for Tests 3 and 4 for reasons previously explained. Rise times of the applied pressures were approximately 3 milliseconds, and the effective decay time varied over the range of 100 to 123 milliseconds. Effective decay time is that time obtained from extending a straight line through the maximum pressure and the value of the pressure at the time of maximum deflection to the time axis on the pressure-time plot. The effective decay time and the rise time may be compared with the times of maximum deflection listed in Table VII to judge whether or not the structure actually "saw" the load as a dynamic loading. Since the ratio of rise time to the time of maximum deflection is about 1 to 6 in each case, there is no question that the structure sensed the blast as a dynamic loading. The loading, however, could not be considered of long duration (as emanates from megaton weapons) because the effective decay time was such that the loading could drop off as much as 20 percent prior to the time the structure reaches its maximum deflection. Therefore, loading with the same peak pressure but longer effective decay time could produce larger deflections, thrusts, and moments than were induced in the test structure.

The time variation of the deflection and other quantities sensed is shown in the oscillograms of Figures 13 and 14. Most of the subsequent plots are for Test 3, which was the first loading to 25 psi; however, the oscillograms given are for Test 4, the second loading to 25 psi. The reason for including the oscillograms for Test 4 is that experience with Test 3 permitted adjustment of attenuations and galvanometer locations to permit near optimum spacing of the traces for visual presentation. This permitted direct reproduction of the oscillograms and avoided loss of detail from retracing and regrouping of the traces. All transducers functioned and the records were of good quality. The magnitude of any quantity at a given time is obtained by multiplying the amplitude of motion from the undisturbed trace line times the attenuation times the calibration factor for the particular transducer. Zero time is taken as the time at which the pressure wave activates the surface pressure gage.

Table VII. Dynamic Test Results; Unshielded Cylinder

Test No.	Peak Crown Pressure (psi)	Effective Decay Time (msec)	Rise Time (msec)	Time to Maximum Deflection (msec)	Peak Deflections (in.)					
					D4 0°	D5 45°	D1 90°	D2 180°	D3 225°	D6 270°
1	9.2	100	3	18	-0.070	0.001	0.086	0.088	0.028	0.073
2	9.2	105	3	18	-0.043	0.001	0.050	0.040	0.013	0.050
3	22.6	123	2	20	-0.124	0.013	0.148	0.138	0.043	0.141
4	26.7	117	3	16	-0.126	0.021	0.134	0.130	0.023	0.138

+ deflection = downward or increase in length of diameter

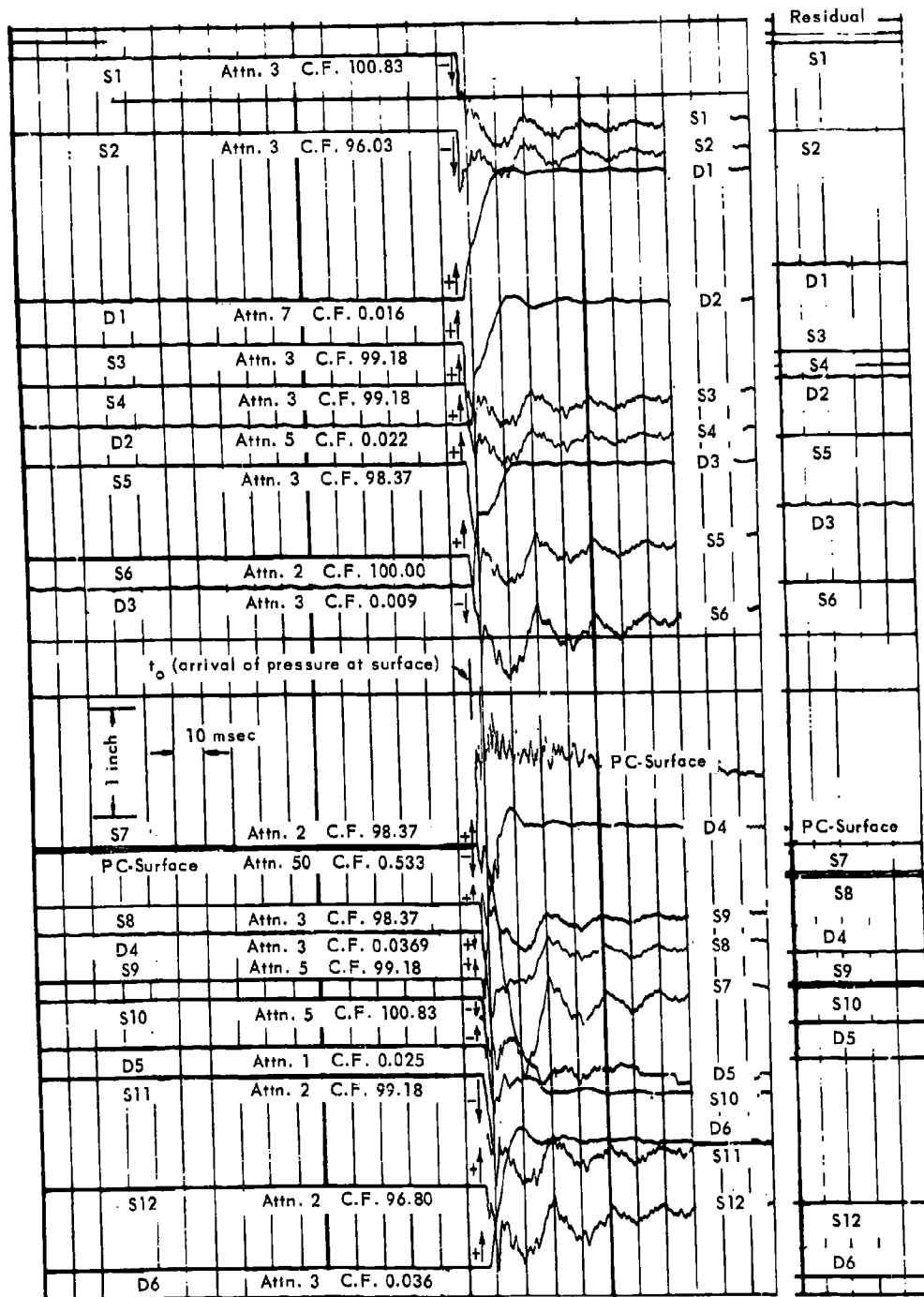


Figure 13. Oscillogram — Dynamic Test 4, 25 psi.

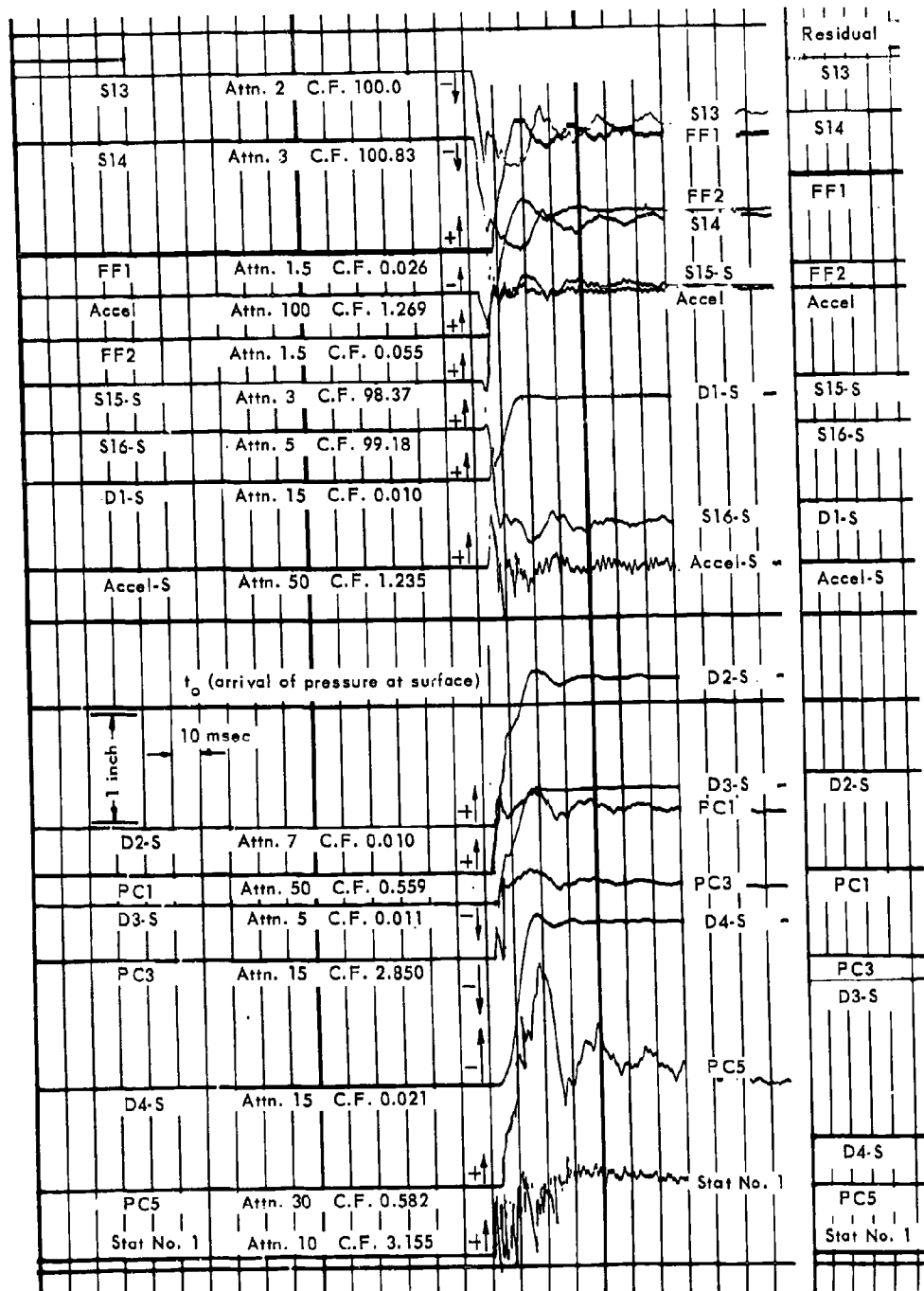


Figure 14. Oscillogram — Dynamic Test 4, 25 psi.

It may be noted from the oscillogram traces that the system is highly damped since even the strains damp out in approximately three cycles. The vibrations of the strain gages and the deflection gages indicate that the natural period of the system is approximately 19 milliseconds. Residual locations of the traces after the load was removed are given at the extreme right of the oscillograms. Data from the oscillograms are plotted in Figures 15 through 26.

Figure 15 gives the deflection distribution of the cylinder at the time of maximum deflection of the crown. These are the deflections experienced by the unshielded cylinder in Test 3, the first loading to 25 psi. Peak values of the deflections at various points around the perimeter are given in Table VII for the four different loadings. The small-magnitude circumferential waves are not shown in Figure 15, which shows only the gross deflected shape. Corresponding thrust and moment distributions computed from the strain data in Table VIII are given in Figures 16 and 17. The thrust at the 90-degree point (Figure 16) is approximately 14 percent greater than the corresponding thrust experienced in the static tests. The thrust distribution, however, is much the same as for the static loading. A plot from the theory for a cylinder in an elastic medium<sup>7</sup> is also shown on Figure 16. The theory and experiment seem to be in reasonably good agreement, although the theoretical values are somewhat less than the corresponding experimentally determined values.

Figure 17 shows the distribution of moments around the cylinder and indicates the form of the circumferential waves which develop around the perimeter. It may be noted that the maximum moment occurred at the bottom of the cylinder and that the period of the circumferential waves was approximately 46 degrees on the sides and 42 degrees on the bottom. A comparison of the experimentally determined moment curve from Figure 17 with the static moment distribution of Figure 11 shows that the moments were larger at the bottom in the static case but had a lesser magnitude elsewhere around the perimeter. Not too much significance can be attached to this comparison since the induced moments are probably quite sensitive to the stresses and deformations induced on the backfilling. Figure 17 shows that the moments predicted from the theory<sup>7</sup> were not close to the moments which actually occur in a thin-walled cylinder. Agreement might be achieved by reworking the theory to include terms which account for the deformed geometry. The shape of the moment distribution was similar at different times even though the magnitude varied with time.

The variation of thrust and moment with time is shown in Figures 18 through 23. Variation of thrust with time was essentially the same at all points around the perimeter except at the 180-degree point; consequently, thrust-time curves are only given for the 90-degree and 180-degree points. It may be seen from Figure 18 that the

thrust rises sharply to a magnitude about three-quarters of its peak value in a time equal to the rise time of the applied overpressure. Thereafter, it increases rather gradually and does not reach its peak value until a time of approximately 15 milliseconds, which is just slightly less than the time to maximum deflection. The thrust at the 90-degree point was 25 percent greater than the product of the surface pressure times the radius (that thrust which would be induced by hydrostatic loading equal in magnitude to the surface overpressure). Values of the quasi-static thrust and residual thrust are indicated on the extreme right of the time axis. The quasi-static values are those which exist immediately after the dynamic response has damped out and the system is, for all practical purposes, in a state of static equilibrium. The residual values, of course, are those remaining after the load is removed from the system. Figure 19 shows that no thrust was induced at the bottom of the cylinder until 2 milliseconds after the pressure wave had arrived at the soil surface. The magnitude of the peak thrust at the 180-degree point was about one-third of the thrust at the 90-degree point. One may observe that the residual thrust was very small in contrast with the residual moments indicated in Figures 20 and 21.

Variation of moment with time was quite different at different points around the perimeter, and the residual moments were quite different from the moments due to backfilling. From Figure 20 it may be seen that the moment at the zero-degree point increased gradually and reached a peak value about the time of maximum deflection, while at the 135-degree point the peak moment was reached in approximately 4 milliseconds and subsequently decayed to essentially zero. Moments at the zero through 135-degree points were small compared with the moment at the 180-degree point, shown in Figure 21, and the latter moment was small compared to the yield moment of the section. Figure 21 shows that the moment near the bottom decreased slightly then increased abruptly to a value near its maximum in about 6 milliseconds. The quasi-static moment at the 180-degree point was even slightly greater than the maximum dynamic value. These values for the unshielded cylinder may be compared with the corresponding quantities for the shielded cylinder shown in Figures 22 through 24.

Comparing the thrust-time curve of Figure 22 with the corresponding curve of Figure 19 for an unshielded cylinder, one observes that the maximum thrust is approximately the same in both cases, although the shape of the function is altered. Again, on comparing the moment-time curve of Figure 23 with the moment-time curve for the unshielded cylinder from Figure 21, it is observed that the maximum moment is the same but that the shape of the function is altered. One would infer from this that the tendency to transitional snap buckling which usually occurs at the bottom of the cylinder<sup>6</sup> would be the same whether or not one uses shielding over the cylinder.

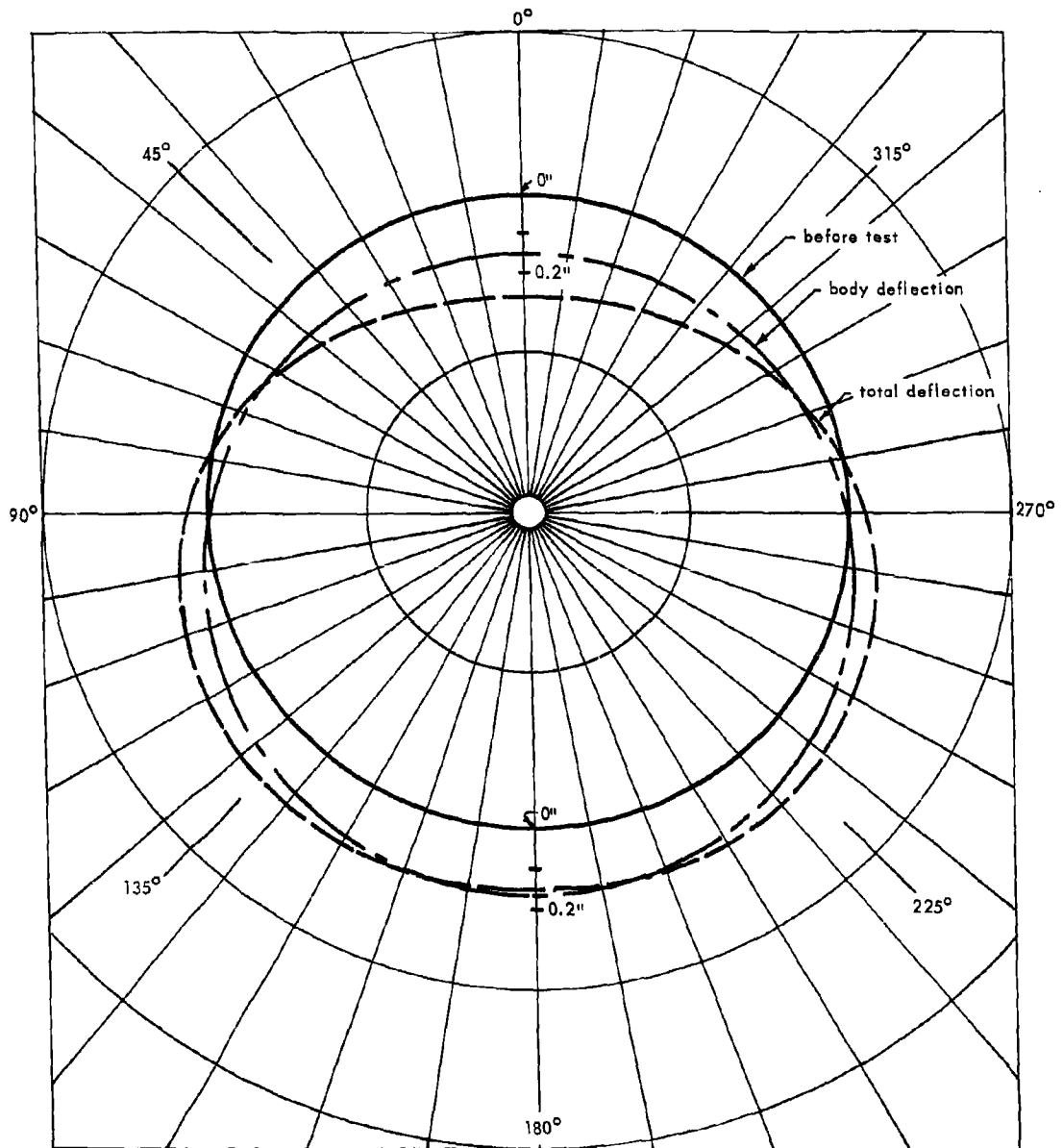


Figure 15. Peak deflection — Dynamic Test 3, 25 psi; unshielded cylinder.

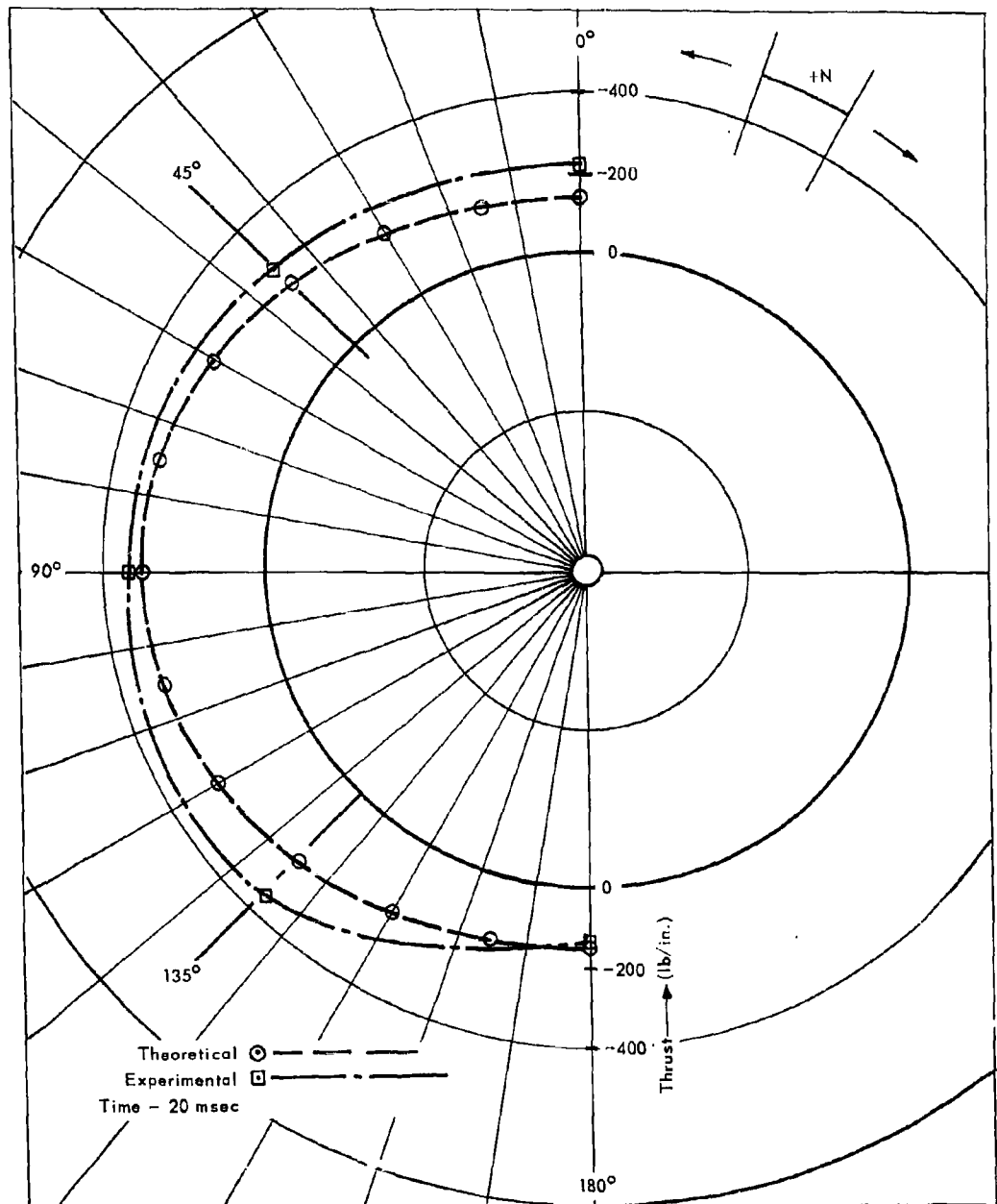


Figure 16. Thrust diagram — Dynamic Test 3, 25 psi; unshielded cylinder.

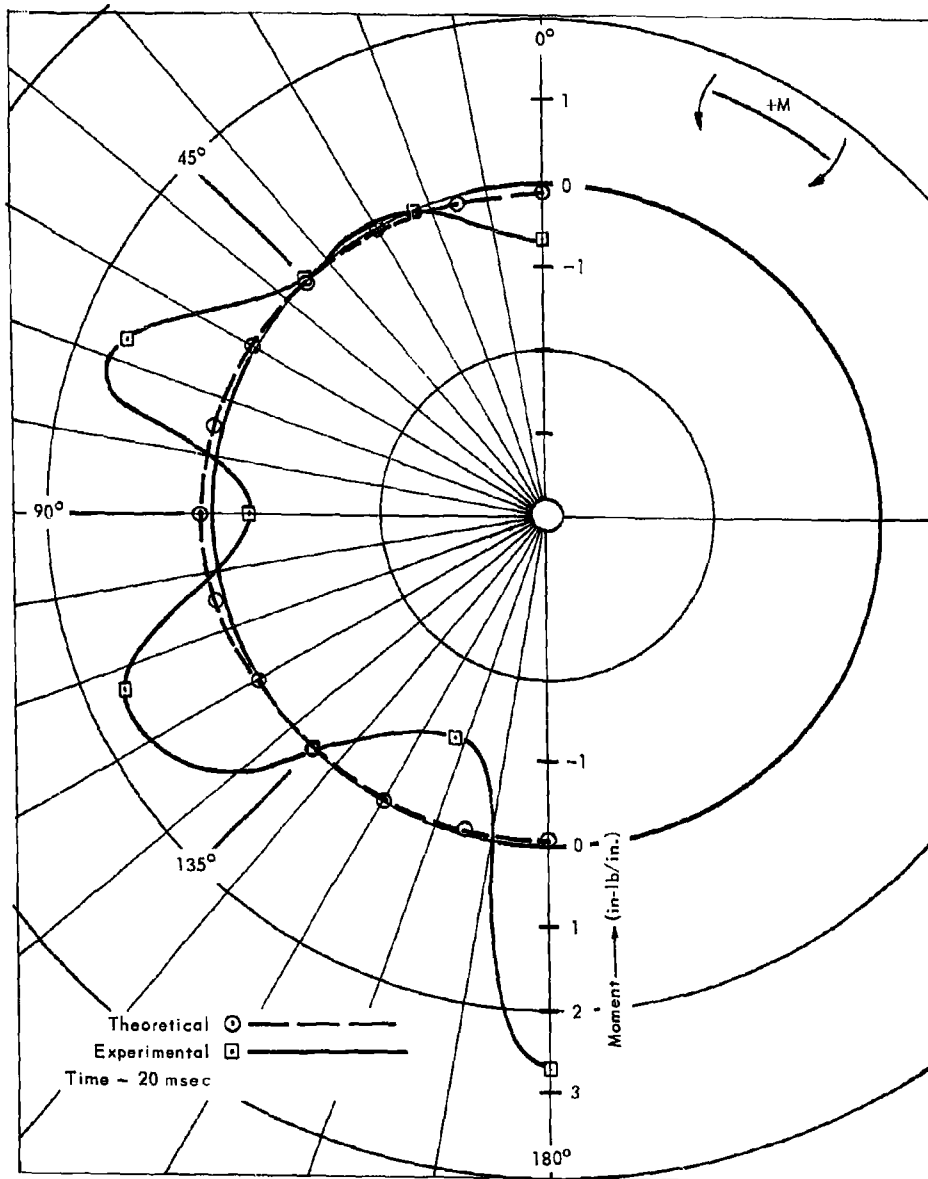


Figure 17. Moment diagram — Dynamic Test 3, 25 psi; unshielded cylinder.

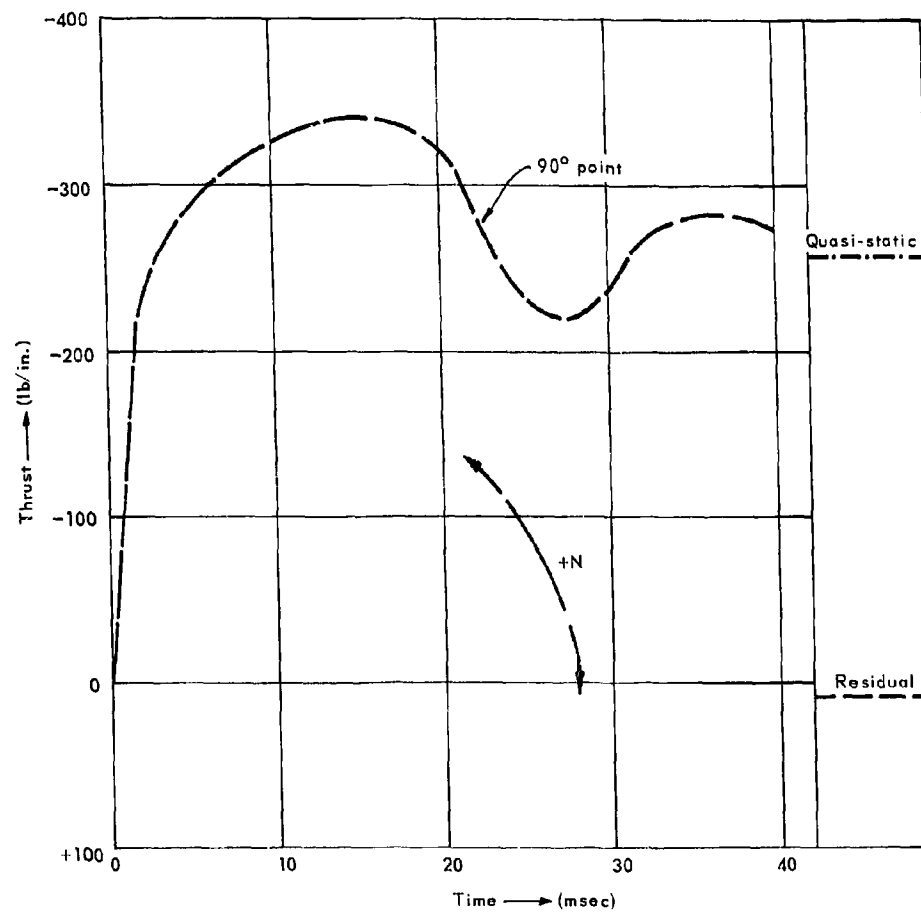


Figure 18. Thrust vs time — Test 3, 90° point; unshielded cylinder.

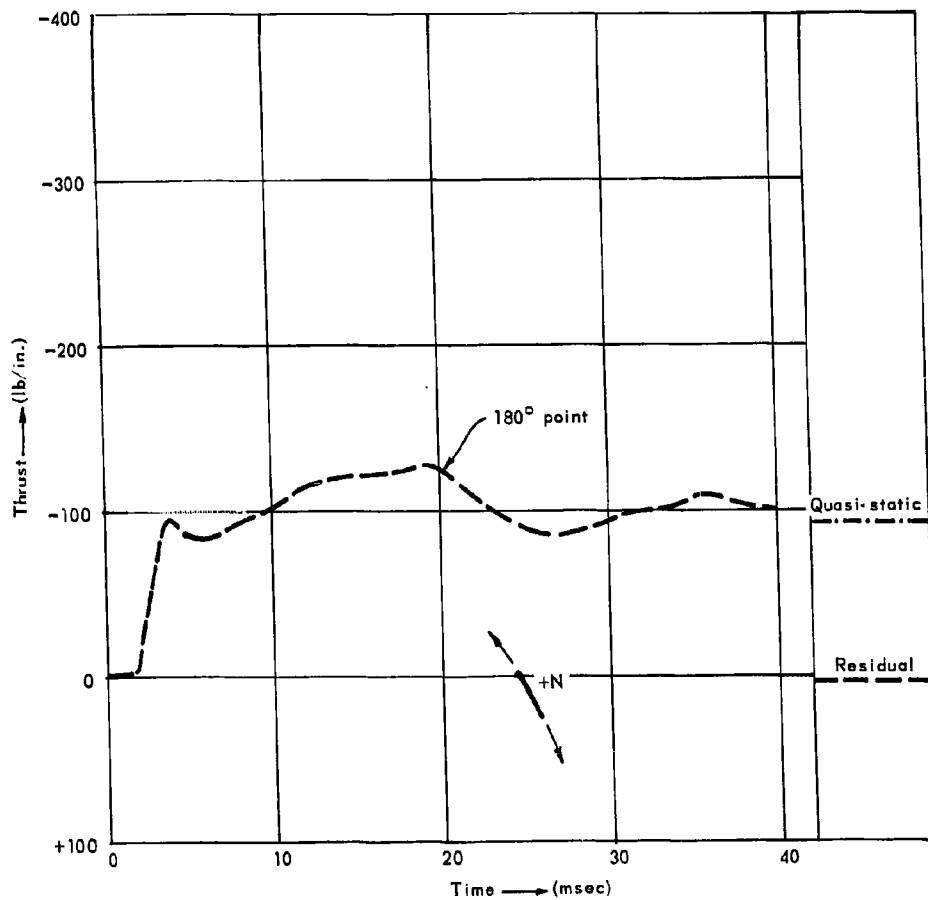


Figure 19. Thrust vs time — Test 3, 180° point; unshielded cylinder.

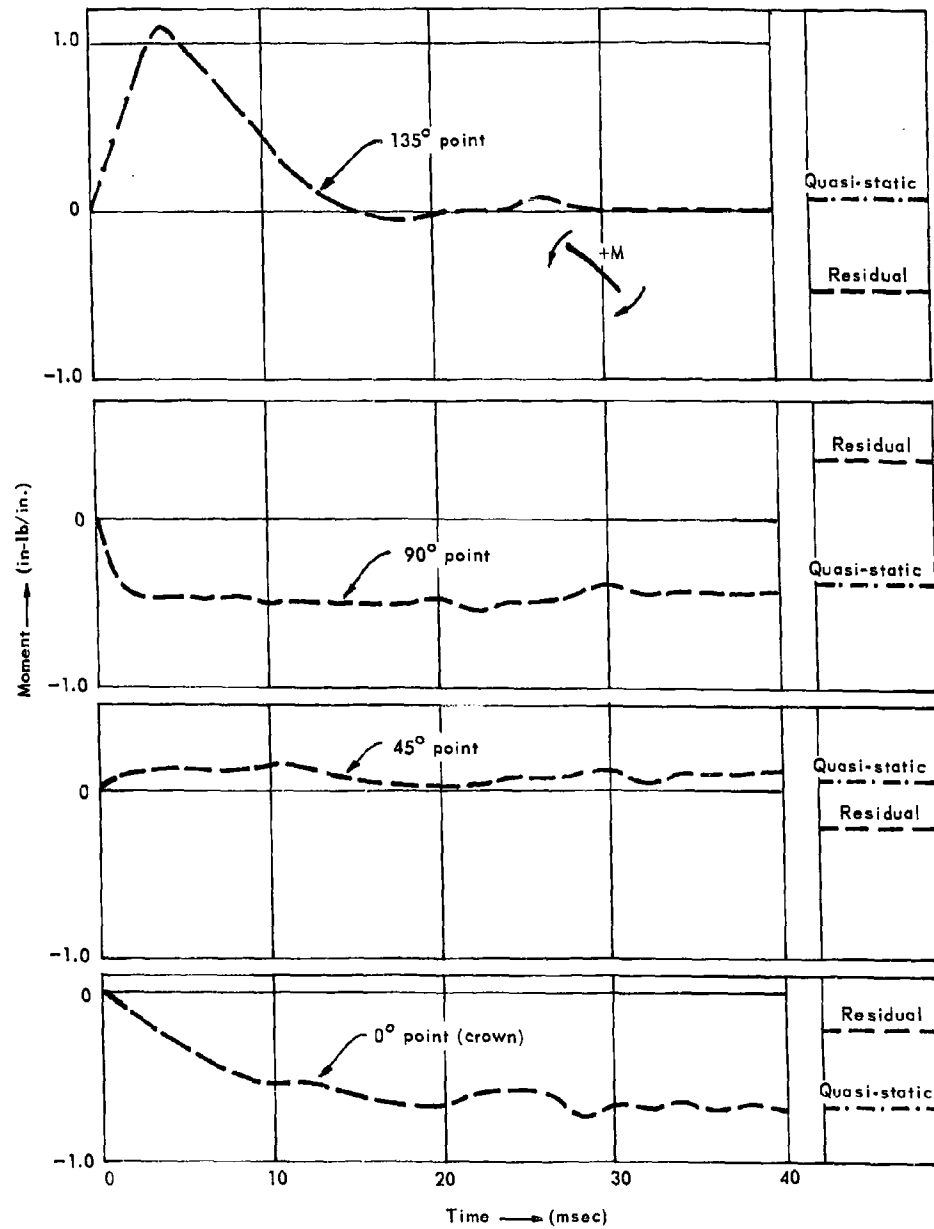


Figure 20. Moment vs time — Test 3; unshielded cylinder.

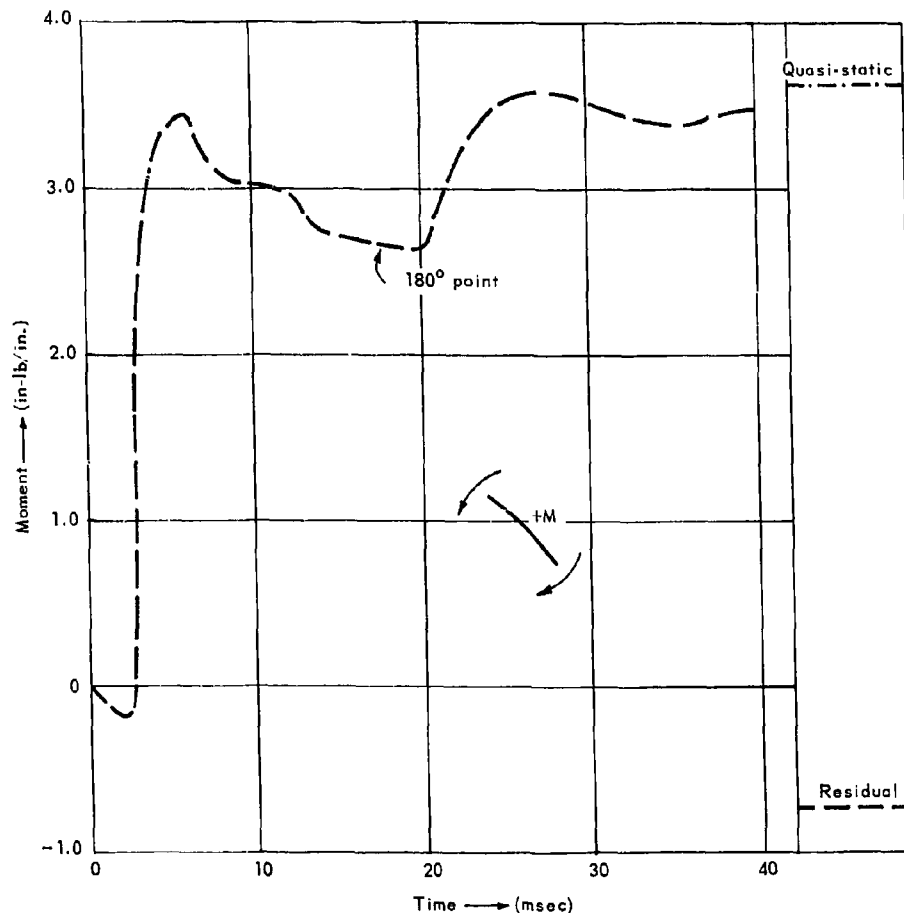


Figure 21. Moment vs time — Test 3, 180° point; unshielded cylinder.

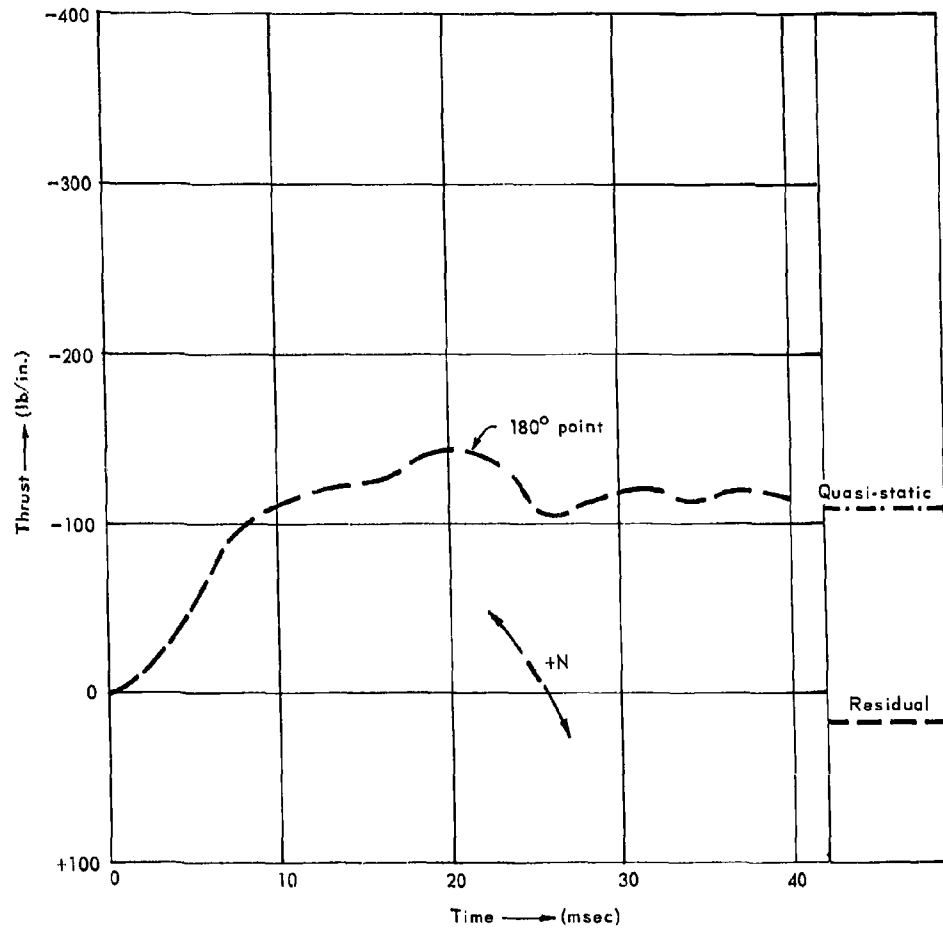


Figure 22. Thrust vs time — Test 3, 180° point; shielded cylinder.

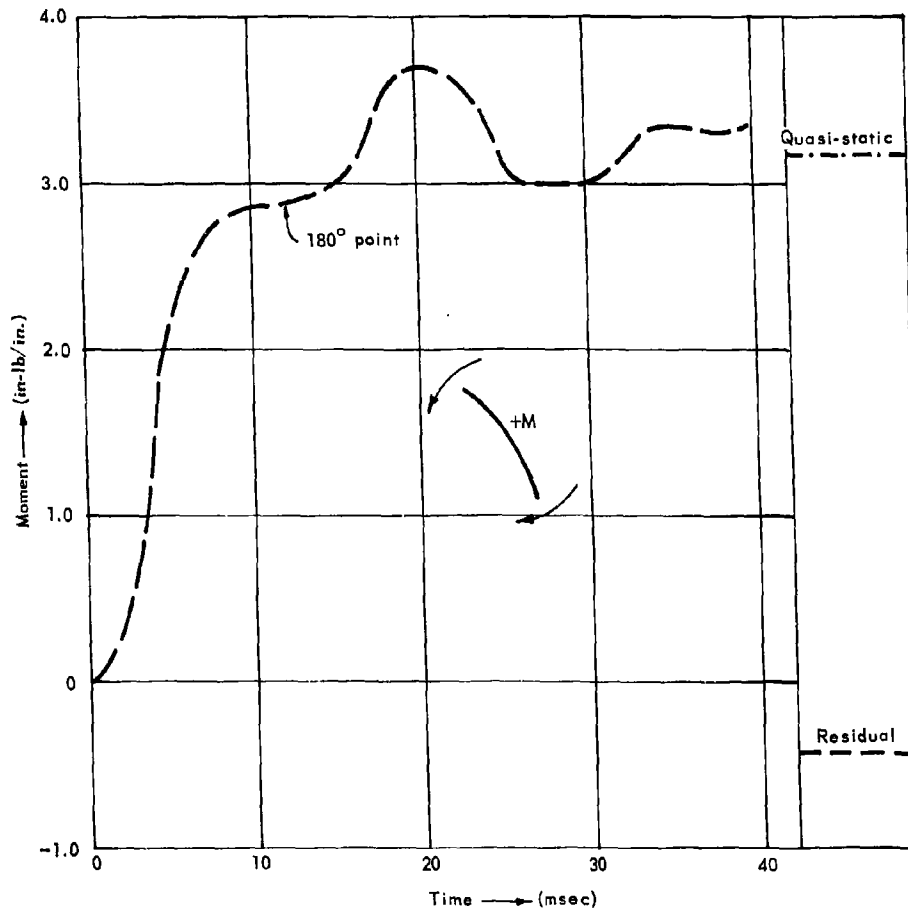


Figure 23. Moment vs time — Test 3, 180° point; shielded cylinder.

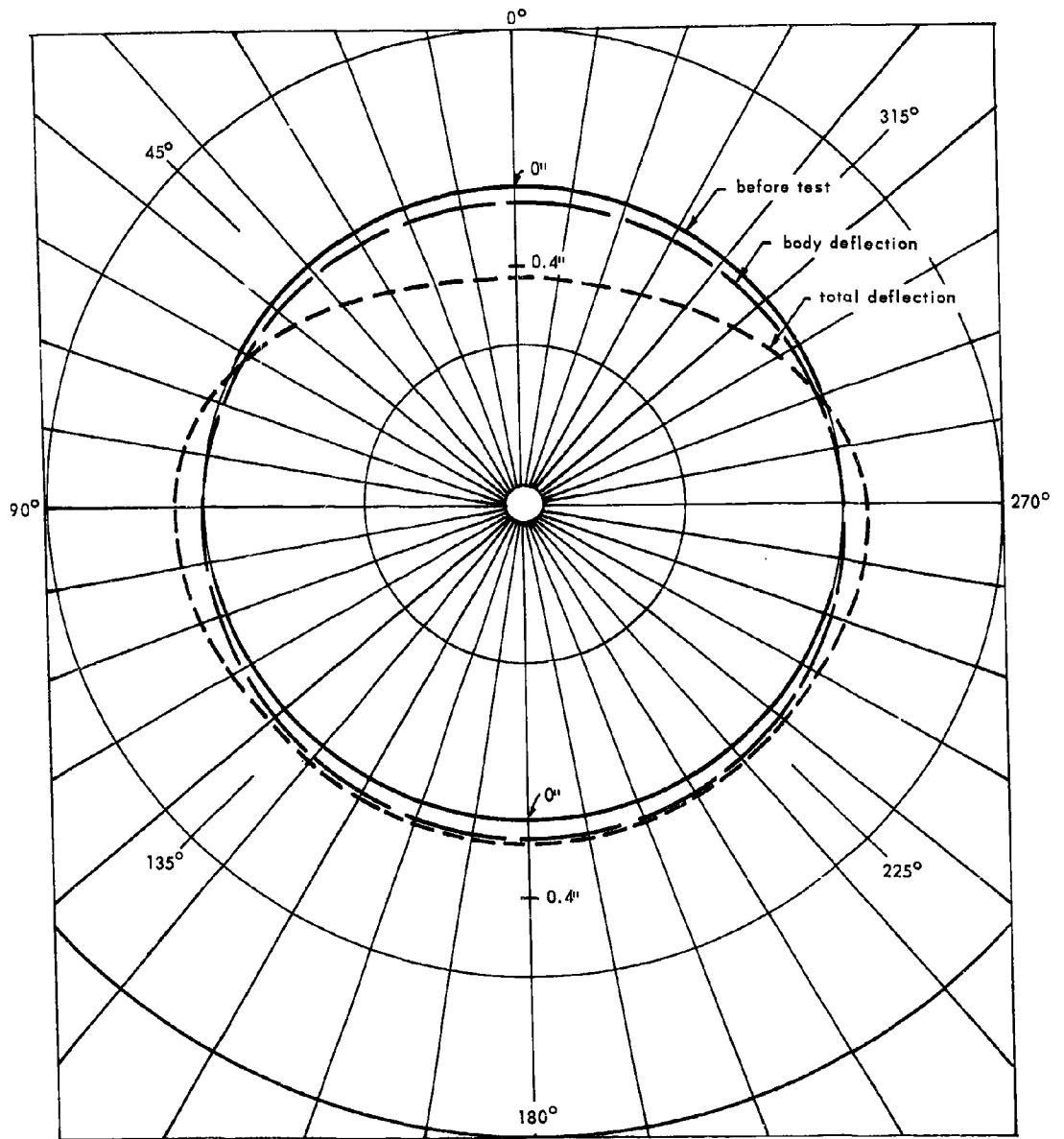


Figure 24. Peak deflection — Dynamic Test 3, 25 psi; shielded cylinder.

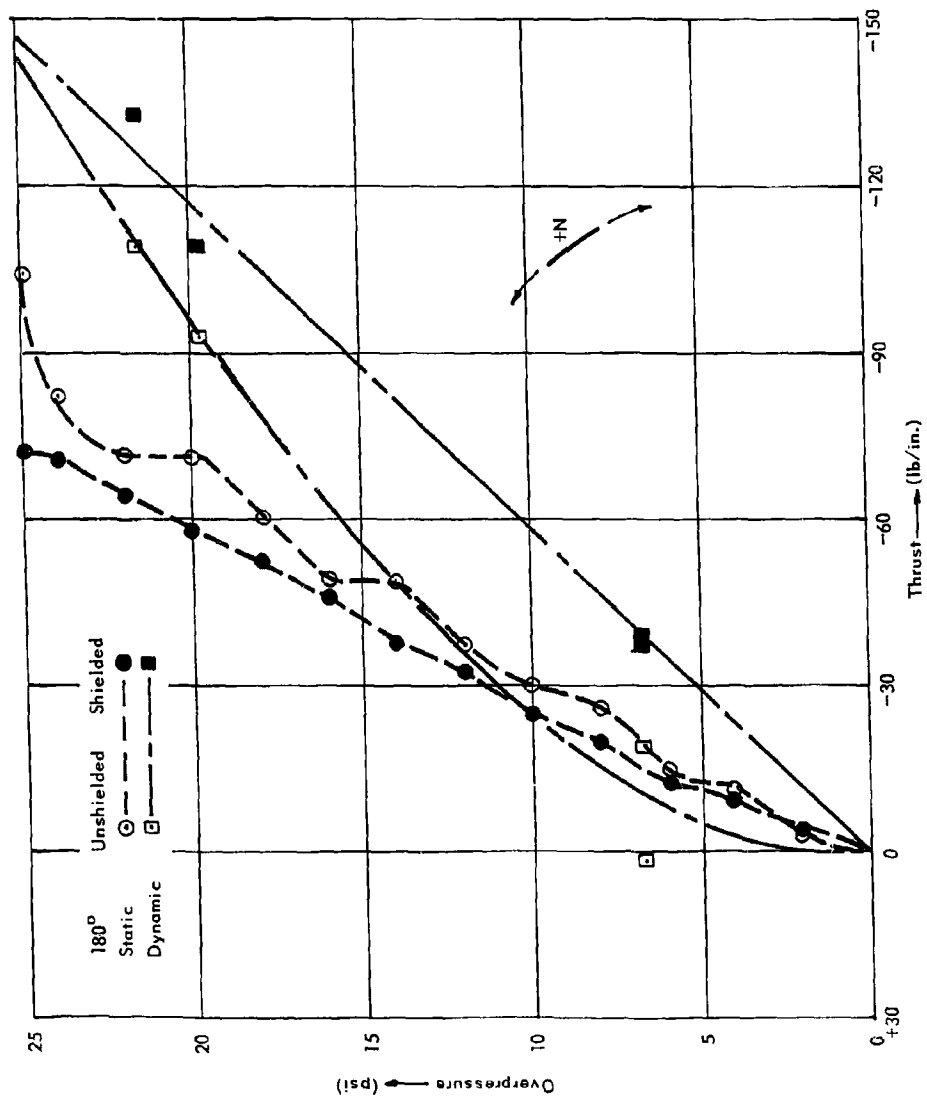


Figure 25. Quasi-static thrust vs overpressure.

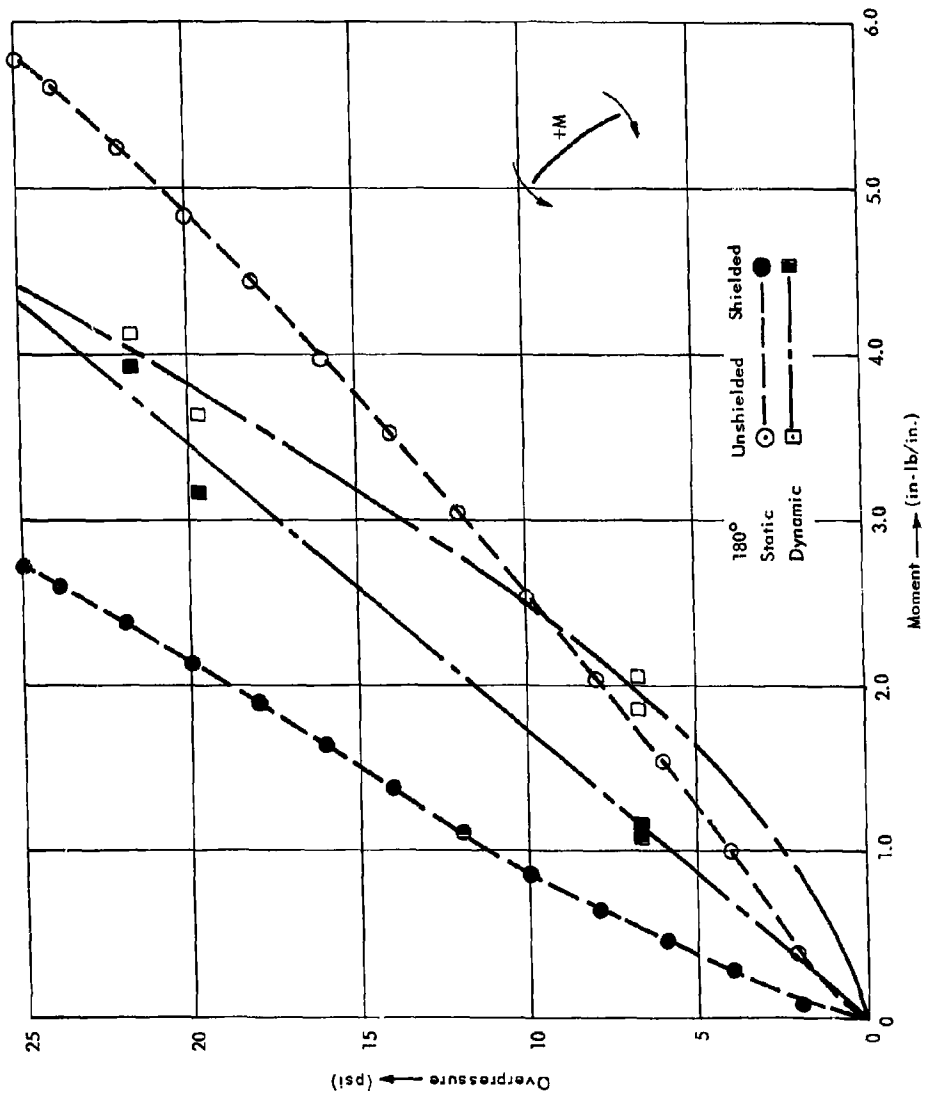


Figure 26. Quasi-static moment vs overpressure.

Table VIII. Peak Strains in Cylinder — Dynamic Tests; Unshielded Cylinder

Test No.	Surface Pressure (psi)	Gage Number													
		1	2	3	4	5	6	7	8	9	10	11	12	13	14
		Maximum Value of Unit Strain ( $\mu$ in./in.)													
1	9.2	-113	-50	-68	-69	-92	-95	-63	-150	205	-252	-68	-19	-36	-164
2	9.2	-131	-47	-97	-99	-121	-67	-26	-128	188	-238	-79	-40	-54	-153
3	22.6	-218	-105	-188	-198	-280	-196	-240	-260	254	-374	-178	-106	-121	-248
4	26.7	-254	-115	-217	-214	-325	-222	-392	-233	342	-575	-196	-132	-174	-306

Negative strain indicates compression.

Note: These peak values did not all occur simultaneously.

The tendency to caving buckling, however, would be appreciably altered. This is deduced by comparing the deflection distribution for the shielded cylinder shown in Figure 24 with the corresponding deflection distribution for the unshielded cylinder in Figure 15. The deflections of the upper portion of the shielded cylinder are almost double the values for the unshielded cylinder, which could result in a large increase in moments and greatly reduce the load at which caving of the roof would occur. The phenomena of caving and transitional buckling are discussed in a companion report.<sup>2</sup>

Accelerations appear to vary approximately linearly with overpressure for both the shielded and unshielded cylinders. Acceleration at the base of the shielded cylinder was approximately 1.2 g per psi while the corresponding acceleration without shielding was approximately 4.5 times greater, or 5.4 g per psi. This difference can be explained by the fact that the shielding material reduced passive arching at the sides of the cylinder, allowing the roof to cave and cushion the impulse of the dynamic loading. Therefore, the presence of isolating material appears desirable except for the danger of a caving-mode failure of the cylinder.

An analysis of a simple model of a shielded buried cylinder is presented in Appendix B. The analysis shows that the effect of placing an isolating material over the structure is to delay the time to maximum load and markedly increase the magnitude of the peak load on the crown. The reason for this is that the isolation material, in crushing, permits the mass of soil over the cylinder to achieve a higher velocity and thus develop a larger momentum which is transmitted to the cylinder. From this study and the experimental results, one would conclude that isolation materials with lower modulus and strength than the soil should not be used over the cylinder. On the other hand, the advantages of using a soft bedding or slip joints in the cylinder to improve the load resistance have long been known.

A further comparison of the behavior of shielded and unshielded cylinders is given in Figures 25 and 26. Figure 25 shows the differences in induced thrust at the 180-degree point for both static and dynamic loading. Figure 26 shows a similar comparison for the moments. Again it is cautioned that the differences in the moments could have been due to slight differences in backfill conditions in the static and dynamic test setups.

Although the interface pressures are the least reliable of all the measurements made, it is interesting to compare the variations in time of the indicated pressures at various points around the cylinder. Traces for PC1 at zero degrees, PC3 at 90 degrees, PC5 at 180 degrees, and the surface pressure are given in Figure 27. It may be noted that the pressure at the crown at the time of maximum deflection was almost exactly equal to the surface pressure at that time. The indicated peak

pressure at the 90-degree point was nearly 31 psi as compared with the peak surface pressure of 22.6 psi. The pressures registered at the bottom of the cylinder were much less than one would expect. The character of the pressure-time traces is more exactly seen from the oscillogram of Figure 14. Contrary to expectations, except for PC5, the interface pressure readings seem quite reasonable.

#### Comparison of Static and Dynamic Response

Interesting comparisons can be made from the data of Tables III and VII. Considering only the values for 25 psi, the various deflections induced by the static and dynamic loads will be compared. Gage D1 provides a measure of the body motion, and it is found that this value was 58 percent greater under dynamic than under static loading. Gages D4 and D6 indicate the basic change in shape or flattening of the cylinder. It is found that under dynamic loading these deflections were of the order of twice the corresponding static values. This would lead one to believe that in the vertical direction the cylinder acts much as a simple spring-mass system where the soil over the cylinder is the mass and the cylinder and its confining soil act as the spring. The soil, of course, also acts as a damper. Downward deflection of the bottom (gage D2) was little different under dynamic or static loading. One may conclude, therefore, that there is a basic difference in the deflections induced under dynamic and static loading. It is highly unlikely that this difference is due to anything but the loading, considering the careful control that was maintained and the essentially equal soil densities achieved in the two test setups. (See Table A-1, Appendix A.)

The thrust distribution for the two load conditions was much the same, and the point of maximum moment was at the cylinder base in all cases. Under the blast load, the peak thrust was approximately 14 percent larger than for static loading; in contrast, the maximum dynamic moment was actually less than the maximum static moment, although the moments on the side and at the crown were somewhat larger.

#### Recapitulation

From the preceding presentation of results and knowledge of other tests,<sup>6</sup> it is clear that static behavior of thin-walled cylinders with shallow burial is characterized by:

1. A body motion and flattening upon which are superimposed circumferential waves.
2. Downward deflection of the crown as the upper portion of the cylinder assumes the form of the first nonextensional symmetrical mode of a two-hinged arch.

3. A reasonably uniform thrust around the perimeter approximately equal to that which would exist under hydrostatic loading of the same magnitude — except that the thrust is reduced considerably at the top and at the bottom.
4. Occurrence of maximum moment in the vicinity of the bottom of the cylinder.

Under dynamic loading, the unshielded cylinder exhibited essentially the same characteristics of behavior. The major differences were that the upper portion of the cylinder experienced deflections of approximately twice those induced from the static loading, and the thrust on the sides was approximately 14 percent greater than under static loading. The differences in deformation behavior and distribution of moment lead one to expect that the caving mode is much more critical under dynamic loading than under static loading, but that the transitional buckling load would be about the same for static and dynamic load conditions.

#### Deficiencies of Work

Experiences with similar tests on buried arches enabled the pursuit and conduct of the buried cylinder tests with essentially no difficulties. Subject to the limitations of knowledge of soil-pressure measurement, the data was generally consistent and is considered of good quality.

As in any experimental program, these tests have their limitations, namely:

1. The tests are limited in number.
2. The attainable magnitude of the peak applied load was much less than desired.
3. Precise information is lacking on the influence of the boundaries of the simulator test pit on the behavior of the soil-structure system.

Tests of the type reported are expensive and time-consuming, thus limiting the number of tests of this type which can be performed. It was considered important in these initial tests to use as large a model as possible to avoid the problems inherent in the use of small models. Now that the data are available, it should be most helpful in judging the results from tests on smaller cylinders which are currently in progress at other organizations, and small-scale tests on cylinders which may subsequently be performed at this laboratory.

The magnitude of the peak load which could be applied was limited by the capability of the test facilities available. Eventually tests of this type should be performed to much higher overpressures where failure can be induced.

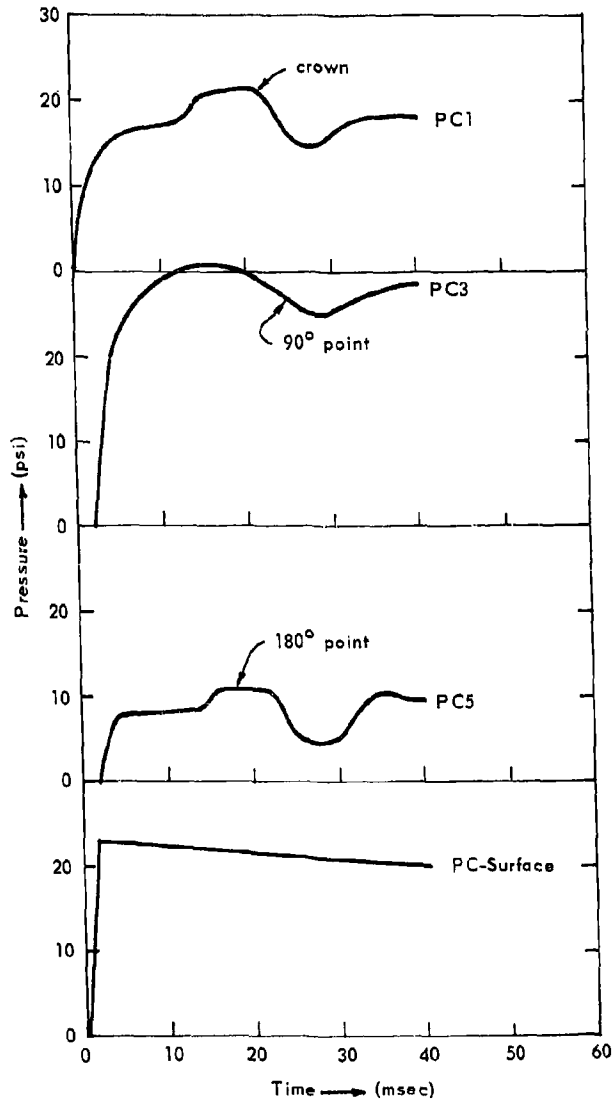


Figure 27. Surface and interface pressures, Test 3.

Available information indicates that the influence of the boundary of the test pit on the behavior of the models would be small. Precise determination of this effect must await development of adequate soil pressure cells. In the interim, the authors believe that the effects of the boundaries would be much less than variations due to soil properties.

## FINDINGS AND CONCLUSIONS

These tests define the general behavior of thin metal cylinders of shallow burial whose axes are parallel to the soil surface and which have static or blast loads uniformly distributed over the soil surface. The form of the deflection, thrust, and moment distribution are found to be much the same under the two types of loading. There are important basic differences, however, as follows:

1. The deflection of the crown (the flattening) of the cylinder under dynamic load was about twice that under static loading.
2. The maximum thrust for dynamic loading was approximately 14 percent greater than for static loading.
3. The maximum moment for static loading was larger than for dynamic loading although the moments on the sides were larger under dynamic loading. The deflection behavior would lead one to expect that the caving mode of failure will be more critical under dynamic loading than under static loading.

A comparison between cylinder behavior with and without a low-modulus, low-strength material in the soil above the cylinder indicates that the advantages of such shielding are problematic. The presence of low-modulus material resulted in undesirable behavior in that the deflections of the crown became larger than they would have been otherwise. On the other hand, the shielding material greatly reduced acceleration of the cylinder base.

The tests form the basis for the conclusion, justified more fully elsewhere,<sup>2</sup> that the net arching across a shallow-buried thin-metal cylinder in a uniform soil field is essentially zero.

## ACKNOWLEDGMENTS

The services of Mr. C. R. White for his counsel concerning the soils aspects of the experiments are gratefully acknowledged. Appreciation is also extended to those who gave their time in reviewing this document.

## REFERENCES

1. U. S. Navy, Bureau of Yards and Docks. Publication P-81: Personnel shelters and protective construction. Washington, D. C., Sept. 1961.
2. U. S. Naval Civil Engineering Laboratory. Technical Report R-344: The behavior of shallow-buried cylinders — A synthesis and extension of contemporary knowledge, by J. R. Allgood. Port Hueneme, Calif. (To be published.)
3. W. A. Shaw and J. R. Allgood. "An atomic blast simulator," Society for Experimental Stress Analysis, Proceedings, vol. 17, no. 1, 1959, pp. 127-134.
4. U. S. Naval Civil Engineering Laboratory. Technical Report R-216: Blast loading of small buried arches, by J. R. Allgood, C. R. White, R. F. Swalley, and H. L. Gill. Port Hueneme, Calif., Apr. 1963.
5. U. S. Naval Civil Engineering Laboratory. Technical Report R-278: Static loading of small buried arches, by H. L. Gill and J. R. Allgood. Port Hueneme, Calif., Jan. 1964.
6. Gt. Brit. Military Engineering Experimental Establishment. Report RES 7/1: Deflection and collapse of buried tubes, by P. S. Bulson. Christchurch, Hampshire, England, Nov. 1962.
7. T. Yoshihara. Interaction of plane elastic waves with an elastic cylindrical shell, Ph D thesis, Department of Civil Engineering, University of Illinois, 1963. See also University of Illinois, Department of Civil Engineering. Structural Research Series SRS-261: Interaction of plane elastic waves with an elastic cylindrical shell, by T. Yoshihara, A. R. Robinson, and J. L. Merritt. Urbana, Ill., 1963.
8. L. S. Jacobsen and R. S. Ayre. Engineering vibrations; with applications to structures and machinery. New York, McGraw-Hill, 1958.

## Appendix A

### SOIL PLACEMENT AND PROPERTIES

The soil used in this test program consisted of a well-graded river-bed sand with a grain-size distribution as shown in Figure A-1 and other physical properties as given in Table A-1. This material, designated NCEL test sand, has been used in all previous soil-structure interaction experiments at NCEL as well as in several other test programs involving soils. It was chosen because of its ready availability and its ease in handling.

At the beginning of this test program, the test pit was already filled with sand from a previous series of static tests of buried arches.<sup>5</sup> This sand was removed to a depth of about 2 feet below what was to be the final elevation of the bottom of the cylinders (about 9 feet) during the static tests and recompacted in 1-foot layers to a depth of 9 inches above the crown of the cylinders. Compaction was achieved by making one pass on each 1-foot layer with a Jackson sled-type vibrator. Four density measurements were then taken and if the densities were not of an adequate uniformity or magnitude, the soil in that layer was loosened and revibrated. This procedure was repeated until the desired densities were attained. These density values were measured by the sand replacement method and are reported in Table A-1.

When the structure elevation was reached, the cylinders, with backfill supports installed, were carefully placed on the surface of the sand and suspended from the simulator so that the dead weight of the structures themselves would not create distortions. The backfill supports shown in Figure 3 were designed to help maintain the true cylindrical configuration of the structures during backfilling. They consisted of a sheet of 1/2-inch-thick plywood measuring approximately 26 inches square with a 24-inch-diameter semicircular cutout on one side. One was placed on the top half of each cylinder. Although there was no support on the bottom half, the high rigidity of the top half with the supports in place greatly reduced the flexibility of the bottom half. It was possible after completion of backfilling to simply pull the supports away from the cylinders and out of the sand without creating any appreciable disturbance to the soil-structure system.

During backfilling beneath the cylinders, it was necessary to hand-place most of the sand to assure a firm seat. Care was taken not to run the Jackson vibrator close enough to the cylinders for its high-force output to create distortions in the structures. Concrete spud vibrators (probe-type) were used in this area to compact the soil. Deflections and strains in the structures were carefully observed to assure that no undesirable distortions of the structures occurred. It was necessary to place blocks between the backfill supports and the blast simulator to keep the cylinders from floating upward during vibration.

Because of the differences in the test setups for the static and dynamic tests, it was necessary to excavate a large amount of soil after completion of the static tests to place the cylinders at the required elevation (about 6 feet) for the dynamic tests. Backfilling and compaction procedures were identical to those for the static tests.

Table A-1. Physical Properties of Soil

Properties	Static Tests	Dynamic Tests
Type of soil	sand	sand
Average unit weight below base of cylinders (before test), lb/ft <sup>3</sup>	113.4	115.1
Average unit weight above base of cylinders (before test), lb/ft <sup>3</sup>	111.4	111.4
Average unit weight above base of cylinders (after test), lb/ft <sup>3</sup>	116.6	108.8
Cohesion, psi	0	0
Moisture content, %	0	0
Specific gravity	2.62	2.62
Seismic velocity, ft/sec		900
Secant modulus of compression <sup>1/</sup> at 25 psi and 114 lb/ft <sup>3</sup> , psi	10,900	10,900

<sup>1/</sup> From consolidometer test

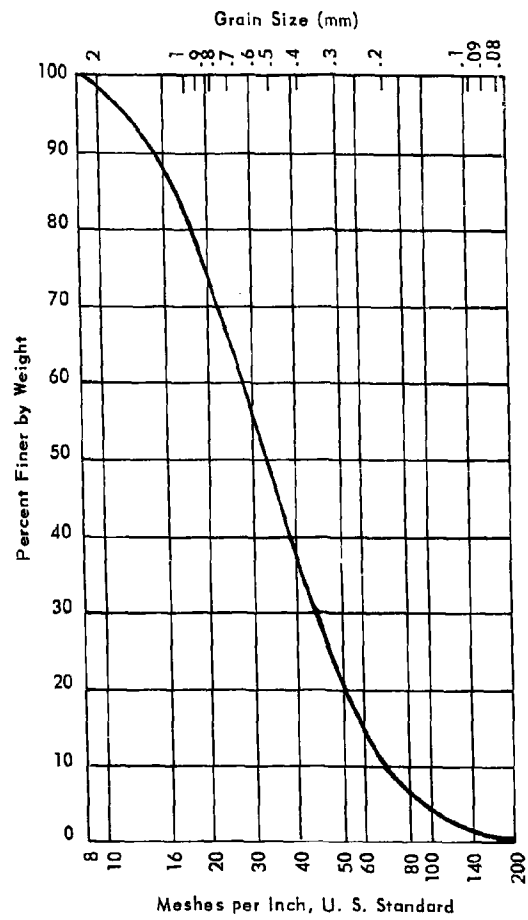


Figure A-1. Grain-size distribution of NCEL test sand.

## Appendix B

### CYLINDER ISOLATION

**PURPOSE.** To investigate the practicality of mechanical shock isolation over buried cylinders.

**APPROACH.** The soil-structure system of Figure B-1a is represented by the model of Figure B-1b. The phase-plane method of solution will be employed.<sup>8</sup> The mathematical notations are defined at the end of the appendix.

**SOLUTION.** Referring to the resistance diagrams of Figure B-1c, considering each range of behavior separately, and neglecting the mass of the structure, the equation of motion becomes

Range 0 - 1

$$m\ddot{x} + \frac{k_1 k_2}{k_1 + k_2} x = p(t) \quad (1)$$

For a step load of magnitude P, Equation 1 becomes

$$\ddot{x} + \omega^2 \left[ x - \frac{(k_1 + k_2)P}{k_1 k_2} \right] = 0$$

Thus,

$$\delta_1 = -\left(\frac{k_1 + k_2}{k_1 k_2}\right)P; \quad \omega^2 = \frac{k_1 k_2}{m(k_1 + k_2)} \quad (2)$$

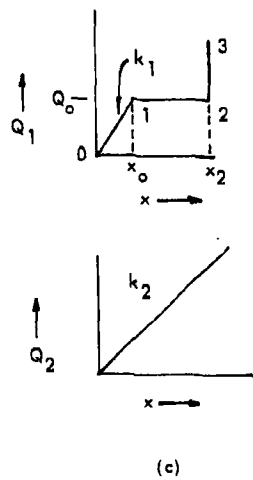
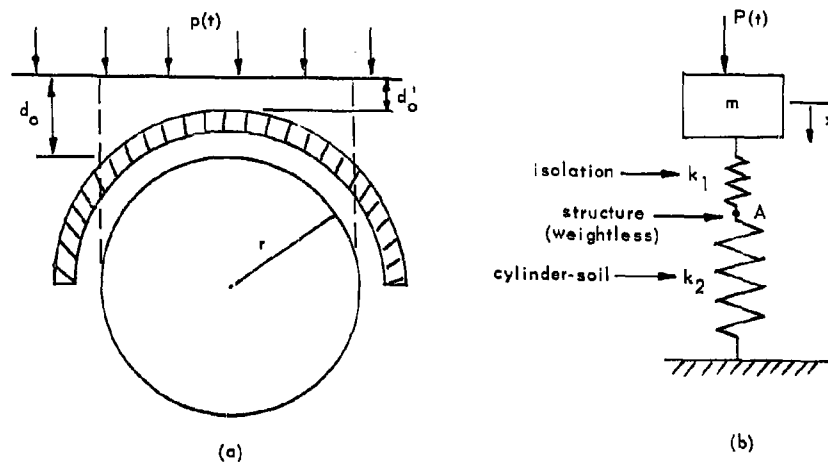


Figure B-1. Buried cylinder and model.

Range 1 - 2

Equation of motion:  $m\ddot{x} + Q_0 = P$

or 
$$\ddot{x} + \omega^2 \left( x - \frac{P - Q_0}{m\omega^2} - x \right) = 0 \quad (3)$$

where  $\omega$  is chosen as per range 0 - 1, and

$$\delta_2 = - \frac{P - Q_0}{m\omega^2} - x \quad (4)$$

Range 2 - 3 (Assume mass acting with the structure =  $2m$ , to account for mass beneath isolation now that it has crushed. Mass used has little effect on peak deflection under a step load.)

Equation of motion:  $2m\ddot{x} + Q_0 + (x - x_2)k_2 = P$

or 
$$\ddot{x} + \omega_3^2 \left( x - \frac{P - Q_0}{k_2} - x_2 \right) = 0 \quad (5)$$

where 
$$\omega_3^2 = \frac{k_2}{2m} \quad (6)$$

and 
$$\delta_3 = - \frac{P - Q_0}{k_2} - x_2 \quad (7)$$

With the preceding equations it is possible to solve a numerical example to demonstrate the effect of placing a low-modulus isolation material in the soil over a buried cylinder.

## NUMERICAL EXAMPLE

### Given:

$$p = 20 \text{ psi}$$

$$k_1 = 4,800 \text{ lb/in.}$$

$$k_2 = 4,560 \text{ lb/in.}$$

$$d_o = 9 \text{ in.}$$

$$d_o' = 5 \text{ in. (depth above isolating material)}$$

$$r = 12 \text{ in.}$$

$$\text{weight of soil} = 110 \text{ lb/ft}^3$$

$$\text{crushing strength of isolation material} = 5 \text{ psi}$$

$$x_o = 0.025 \text{ in.}$$

$$x_2 = 1 \text{ in.}$$

### Calculated Constant Terms:

$$m = \frac{110(5)(24)(1)}{1728(386.4)} = 0.0198 \text{ lb-sec}^2/\text{in.}$$

$$P = 20(24)(1) = 480 \text{ lb}$$

$$Q_o = 5(24)(1) = 120 \text{ lb}$$

### Range 0 - 1

$$\omega^2 = \frac{k_1 k_2}{m(k_1 + k_2)} = \frac{4800(4560)}{0.0198(4800 + 4560)} = 118,100$$

$$\omega = 344 \text{ rad/sec}$$

$$\delta_1 = -\frac{(k_1 + k_2)P}{k_1 k_2} = -\frac{(4800 + 4560)480}{4800(4560)} = -0.205 \text{ in.}$$

Range 1 - 2

$$\delta_2 = -x - \frac{P - Q_o}{m\omega^2} = -x - \frac{480 - 120}{0.0198(118,100)} = -x - 0.1541$$

$$\omega_2 = \omega$$

$$x_L = \frac{Q_o}{k_2} + x_2 = \frac{120}{4560} + 1.00 = 1.026 \text{ in.}$$

Range 2 - 3

$$\omega_3^2 = \frac{k_2}{2m} = \frac{4560}{2(0.0198)} = 115,200$$

$$\omega_3 = 340 \text{ rad/sec}$$

$$\delta_3 = -\frac{P - Q_o}{k_2} - x_2 = -\frac{480 - 120}{4560} - 1 = -1.079 \text{ in.}$$

With the values of  $\delta$  computed above, a phase-plane solution may be generated as shown in Figure B-2.

From the phase-plane solution,  $x_m = 1.635$  inches. The maximum force at the point A (i.e., on the structure) is, therefore,

$$F = Q_o + k_2 x_3$$

where  $x_3 = x_m - x_2 = 1.635 - 1.00 = 0.635$  in.

$$F = 120 + 4560(0.635) = 3016 \text{ lb}$$

Hence,

$$\frac{F}{P} = \frac{3016}{480} = 6.28$$

**CONCLUSION.** From the preceding, it is evident that the effect of the isolating material is to markedly increase the magnitude of the peak load on the structure. Apparently, the isolating material produces a deleterious effect rather than a helpful one.

#### SYMBOLS

- $d_o$  Depth of soil cover over crown of cylinder
- $F$  Maximum force on structure
- $k_1$  Initial spring constant of isolating material
- $k_2$  Spring constant of soil-cylinder combination
- $m$  Accelerated mass

$P$	Magnitude of step load
$p$	Surface overpressure
$p(t)$	Pressure as a function of time
$Q_0$	Load at which isolating material yields
$Q_1$	Load reaching isolating material
$Q_2$	Load reaching soil-cylinder combinations
$r$	Radius of cylinder
$x$	Vertical displacement of mass, $m$
$x_L$	Total deflection at end of range 1 - 2
$x_m$	Maximum displacement
$x_0$	Deflection at which isolating material yields
$x_2$	Crushable thickness of isolating material
$x_3$	Deflection of structure
$\delta$	Deflection term
$\omega$	Frequency of system

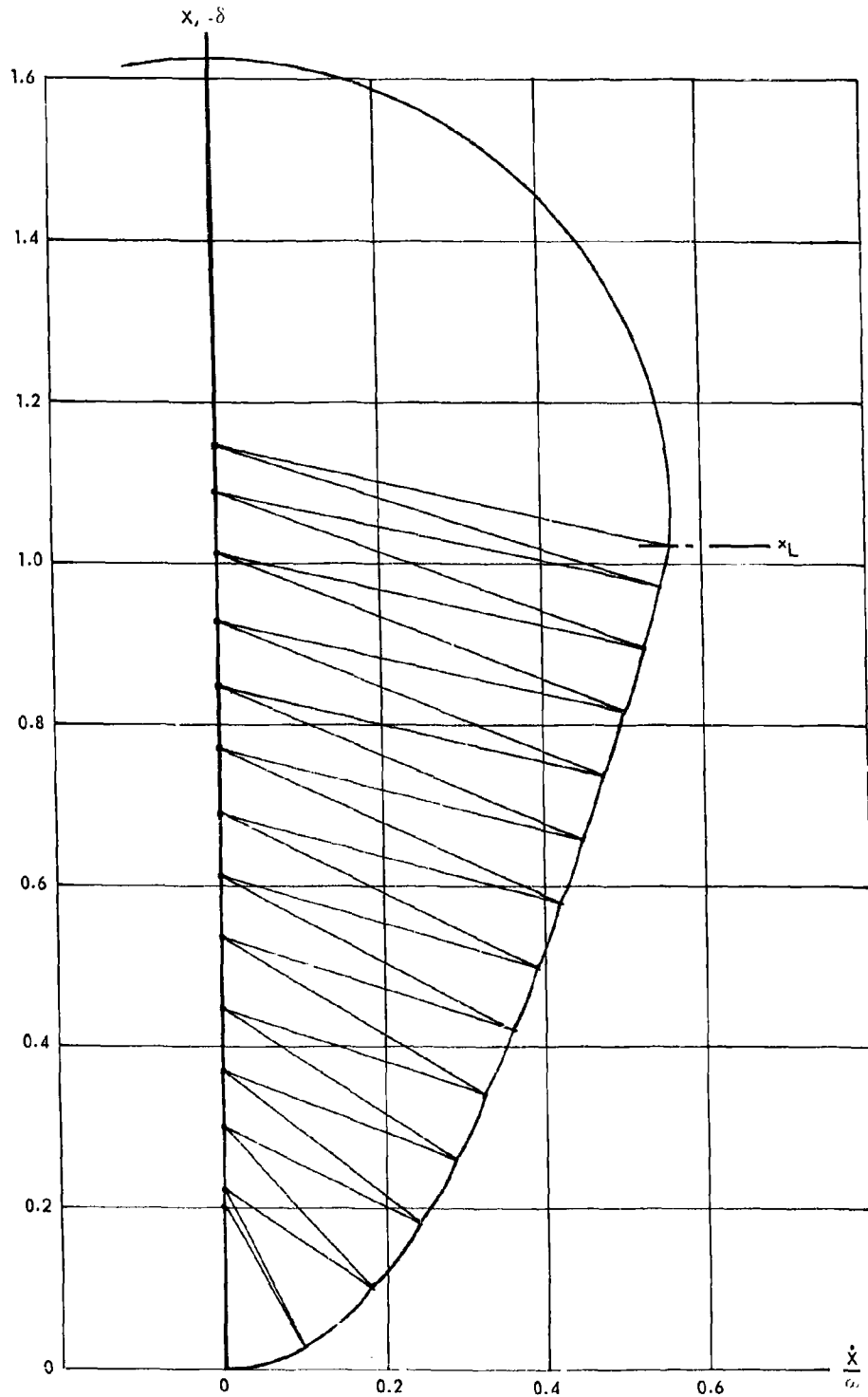


Figure B-2. Phase-plane solution.

DISTRIBUTION LIST

SNDL Code	No. of Activities	Total Copies	
	1	25	Chief, Defense Atomic Support Agency, Washington, D. C.
	1	10	Chief, Bureau of Yards and Docks (Code 42)
23A *	1	1	Naval Forces Commanders (Taiwan only)
39B	2	2	Construction Battalions
39D	5	5	Mobile Construction Battalions
39E	3	3	Amphibious Construction Battalions
39F	1	2	Construction Battalion Base Units
A2A	1	1	Chief of Naval Research - Only
A3	2	2	Chief of Naval Operation (OP-07, OP-04)
A5	5	5	Bureaus
B3	2	2	Colleges
E4	1	2	Laboratory ONR (Washington, D. C. only)
E5	1	1	Research Office ONR (Pasadena only)
E16	1	1	Training Device Center
F9	7	7	Station - CNO (Boston; Key West; San Juan; Long Beach; San Diego; Treasure Island; and Rodman, C. Z. only)
F17	6	6	Communication Station (San Juan; San Francisco; Pearl Harbor; Adak, Alaska; and Guam only)
F41	1	1	Security Station
F42	1	1	Radio Station (Oso and Cheltenham only)
F48	1	1	Security Group Activities (Winter Harbor only)
F61	2	2	Naval Support Activities (London and Naples only)
F77	1	1	Submarine Base (Groton, Conn. only)
F81	2	2	Amphibious Bases
H3	7	7	Hospital (Chelsea; St. Albans, Portsmouth, Va.; Beaufort; Great Lakes; San Diego; and Camp Pendleton only)
H6	1	1	Medical Center
J1	2	2	Administration Command and Unit - BuPers (Great Lakes and San Diego only)
J3	1	1	U. S. Fleet Anti Air Warfare Training Center (Virginia Beach only)
J19	1	1	Receiving Station (Brooklyn only)
J34	1	1	Station - BuPers (Washington, D. C. only)

## DISTRIBUTION LIST (Cont'd)

SNDL Code	No. of Activities	Total Copies	
J46	1	1	Personnel Center
J48	1	1	Construction Training Unit
J60	1	1	School Academy
J65	1	1	School CEC Officers
J84	1	1	School Postgraduate
J90	1	1	School Supply Corps
J95	1	1	School War College
J99	1	1	Communication Training Center
L1	11	11	Shipyards
L7	4	4	Laboratory - BuShips (New London; Panama City; Carderock; and Annapolis only)
L26	5	5	Naval Facilities - BuShips (Antigua; Turks Island; Barbados; San Salvador; and Eleuthera only)
L42	2	2	Fleet Activities - BuShips
M27	4	4	Supply Center
M28	6	6	Supply Depot (except Guantanamo Bay; Subic Bay; and Yokosuka)
M61	2	2	Aviation Supply Office
N1	6	18	BuDocks Director, Overseas Division
N2	9	27	Public Works Offices
N5	3	9	Construction Battalion Center
N6	5	5	Construction Officer-in-Charge
N7	1	1	Construction Resident-Officer-in-Charge
N9	6	12	Public Works Center
N14	1	1	Housing Activity
R9	2	2	Recruit Depots
R10	2	2	Supply Installations (Albany and Barstow only)
R20	1	1	Marine Corps Schools (Quantico)
R64	3	3	Marine Corps Base
R66	1	1	Marine Corps Camp Detachment (Tengan only)
W1A1	6	6	Air Station
W1A2	35	35	Air Station
W1B	8	8	Air Station Auxiliary

DISTRIBUTION LIST (Cont'd)

SNDL Code	No. of Activities	Total Copies	
WIC	3	3	Air Facility (Phoenix; Naha; and Naples only)
WIE	6	6	Marine Corps Air Station (except Quantico)
WIH	9	9	Station - BuWeps (except Rota)
	1	1	Deputy Chief of Staff, Research and Development, Headquarters, U. S. Marine Corps, Washington, D. C.
	1	1	President, Marine Corps Equipment Board, Marine Corps School, Quantico, Va.
	1	1	Chief of Staff, U. S. Army, Chief of Research and Development, Department of the Army, Washington, D. C.
	1	1	Office of the Chief of Engineers, Assistant Chief of Engineering for Civil Works, Department of the Army, Washington, D. C.
	1	1	Chief of Engineers, Department of the Army, Washington, D. C., Attn: Engineering Research and Development Division
	1	1	Chief of Engineers, Department of the Army, Washington, D. C., Attn: ENGCW-OE
	1	3	Headquarters, U. S. Air Force, Directorate of Civil Engineering, Washington, D. C., Attn: AFOCE-ES
	1	1	Commanding Officer, U. S. Naval Construction Battalion Center, Port Hueneme, Calif., Attn: Materiel Dept., Code 140
	1	1	Deputy Chief of Staff, Development, Director of Research and Development, Department of the Air Force, Washington, D. C.
	1	1	Director, National Bureau of Standards, Department of Commerce, Connecticut Avenue, Washington, D. C.
	1	2	Office of the Director, U. S. Coast and Geodetic Survey, Washington, D. C.
	1	20	Defense Documentation Center, Building 5, Cameron Station, Alexandria, Va.
	1	2	Director of Defense Research and Engineering, Department of Defense, Washington, D. C.
	1	2	Director, Bureau of Reclamation, Washington, D. C.
	1	1	Facilities Officer, Code 108, Office of Naval Research, Washington, D. C.
	1	1	Federal Aviation Agency, Office of Management Services, Administrative Services Division, Washington, D. C., Attn: Library Branch

DISTRIBUTION LIST (Cont'd)

No. of Activities	Total Copies	
1	2	Commander Naval Beach Group Two, U. S. Naval Amphibious Base, Little Creek, Norfolk, Va.
1	1	Commander, Pacific Missile Range, Technical Documentation Section, P. O. Box 10, Point Mugu, Calif., Attn: Code 4332
1	2	U. S. Army Engineer Research and Development Laboratories, Attn: STINFO Branch, Fort Belvoir, Va.
1	1	Director, U. S. Naval Ordnance Laboratory, White Oak, Silver Springs, Md.
1	1	Office of Naval Research, Branch Office, Navy No. 100, Box 39, FPO, New York
1	1	U. S. Naval Radiological Defense Laboratory, San Francisco
1	1	Officer in Charge, CECOS, Port Hueneme, Calif., Attn: ADCE Course
1	1	U. S. Air Force, Asst. Chief of Staff, Intelligence, Building B, AHS, Washington, D. C., Attn: Mr. Sargent White
1	1	Commander, Air Force Ballistic Missile Division, Air Research and Development Command, P. O. Box 262, Inglewood, Calif.
1	1	Directorate of Research, Air Force Weapons Laboratory, Kirtland Air Force Base, N. M.
1	1	Office of the Chief of Engineers, Department of the Army, T-7, Gravelly Point, Washington, D. C., Attn: ENGNB
1	1	Commanding Officer, Engineer Research and Development Laboratories, Fort Belvoir, Va.
1	1	Office of the Chief of Engineers, Department of the Army, T-7, Gravelly Point, Washington, D. C., Attn: ENG MC-EB
1	1	Director, U. S. Army Engineer Waterways Experiment Station, P. O. Box 631, Vicksburg, Miss., Attn: Mr. G. L. Arbuthnot, Jr.
1	1	U. S. Army Chemical Center, Nuclear Defense Laboratory, Edgewood, Md.
1	1	Director, Ballistic Research Laboratories, Aberdeen, Md.
1	2	Chief, Defense Atomic Support Agency, Washington, D. C.
1	1	Headquarters, Field Command, Defense Atomic Support Agency, Sandia Base, Albuquerque, N. M.
1	1	U. S. Atomic Energy Commission, Technical Information Service, P. O. Box 62, Oak Ridge, Tenn.
1	1	Director, Civil Effects Test Group, Atomic Energy Commission, Washington, D. C.
1	1	Formulation and Analysis Branch, Mathematics and Computation Laboratory, National Resource Evaluation Center, Office of Emergency Planning, Washington, D. C.
1	2	Library of Congress, Washington, D. C.

DISTRIBUTION LIST (Cont'd)

No. of Activities	Total Copies	
1	1	Disaster Recovery Training Officer, Code 450, Construction Battalion Center, Davisville, R. I.
1	1	Mr. William J. Taylor, Terminal Ballistics Laboratory, Aberdeen Proving Ground, Md.
1	1	LCDR Charles W. Gulick, Jr., CEC, USN, Navy No. 926, FPO, San Francisco
1	1	CDR J. C. LeDoux, Office of Civil Defense, Department of Defense, Washington, D. C.
1	1	CAPT W. M. McLellan, CEC, USN, Ret., 468 1st Street, Albany, N. Y.
1	1	LT Edward S. Perry, U. S. Naval Reserve Officers Training Corps Unit, University of Illinois, Urbana, Ill.
1	1	CAPT L. N. Saunders, CEC, USN, Code C10, U. S. Naval Construction Battalion Center, Port Hueneme, Calif.
1	1	CDR E. M. Saunders, CEC, USN, Chief of Naval Materiel, Department of the Navy, Washington, D. C.
1	1	CDR H. E. Stephens, CEC, USN, Bureau of Yards and Docks, Code 41.101, Washington, D. C.
1	1	LCDR R. C. Vance, CEC, USN, Logistics Director, U. S. Naval Civil Engineering Laboratory, Port Hueneme, Calif.
1	1	CDR W. A. Walls, CEC, USN, Disaster Control Division, Bureau of Yards and Docks, Washington, D. C.
1	1	LT COL Charles D. Daniel, USA, Defense Atomic Support Agency, Washington, D. C.
1	1	Mr. L. Neal FitzSimons, Office of Civil Defense, Department of Defense, Washington, D. C.
1	1	Mr. Ben Taylor, Office of Civil Defense, Department of Defense, Washington, D. C.
1	1	Mr. Charles M. Eisenhower, Radiation Physics Laboratory, National Bureau of Standards, Washington, D. C.
1	1	Mr. O. H. Hill, Building 12, Room 505, Radiation Physics Division, National Bureau of Standards, Washington, D. C.
1	1	CDR J. D. Andrews, CEC, USN, SHAPE Headquarters, APO 55, New York
1	1	CAPT W. J. Christensen, CEC, USN, U. S. Naval Civil Engineering Laboratory, Port Hueneme, Calif.
1	1	CDR J. F. Dobson, CEC, USN, U. S. Naval School, CEC Officers, Port Hueneme, Calif.
1	1	LCDR O. L. Dixon, CEC, USN, U. S. Naval School, CEC Officers, Port Hueneme, Calif.
1	1	LCDR N. W. Clements, CEC, USN, Navy Nuclear Power Unit, Fort Belvoir, Va.
1	1	CDR C. Curione, CEC, USN, Resident Officer-In-Charge-Of-Construction, Long Beach Area, P. O. Box XX, Seal Beach, Calif.

DISTRIBUTION LIST (Cont'd)

No. of Activities	Total Copies	
1	1	LT L. K. Donovan, CEC, USN, U. S. Naval Communication Station, Navy No. 85, FPO, San Francisco
1	1	LT Walter J. Eager, Jr., CEC, USN, Naval Postgraduate School, Monterey, Calif.
1	1	LTJG Clinton W. Kelly, III, CEC, USN, Bureau of Yards and Docks, Program Officer, U. S. Naval Radiological Defense Laboratory, San Francisco
1	1	CDR W. J. Francy, CEC, USN, Bureau of Yards and Docks, Director, Southeast Division, U. S. Naval Base, Charleston, S. C.
1	1	CDR C. F. Krickenberger, CEC, USN, Bureau of Yards and Docks, Code 50.200, Washington, D. C.
1	1	Dr. Lauriston S. Taylor, Chief, Radiation Physics Division, National Bureau of Standards, Washington, D. C.
1	1	Dr. James O. Buchanan, Research Directorate, Office of Civil Defense, Washington, D. C.
1	1	LT S. H. Mathes, CEC, USN, U. S. Naval Construction Battalion Center, Port Hueneme, Calif.
1	1	Mr. Jack C. Greene, Office of Civil Defense, Department of Defense, Washington, D. C.
1	1	Dr. Harold A. Knapp, Fallout Studies Branch, Division of Biology and Medicine, U. S. Atomic Energy Commission, Washington, D. C.
1	1	Dr. Karl Z. Morgan, Director, Health Physics Division, Oak Ridge National Laboratory, Oak Ridge, Tenn.
1	1	Dr. Joseph D. Coker, National Resource Evaluation Center, Executive Office Building, Washington, D. C.
1	1	Dr. Charles F. Ksanda, Military Evaluation Division, U. S. Naval Radiological Defense Laboratory, San Francisco
1	1	Mr. John Auxier, Oak Ridge National Laboratory, Oak Ridge, Tenn.
1	1	Dr. William Kreger, Naval Radiological Defense Laboratory, San Francisco
1	1	Dr. Hans Tiller, Nuclear Defense Laboratory, Army Chemical Center, Md.
1	1	Mr. Irving Gaskill, National Resource Evaluation Center, Executive Office Building, Washington, D. C.
1	1	Mr. George Sisson, Office of Civil Defense, Department of Defense, Washington, D. C.
1	1	Mr. James C. Pettee, National Resource Evaluation Center, Executive Office Building, Washington, D. C.
1	1	LTCOL Russell J. Hutchinson, 052921, Office of the Engineer, Camp Wolters, Mineral Wells, Tex.
1	1	LCDR I. D. Crowley, CEC, USN, Blast and Shock Division, Defense Atomic Support Agency, Washington, D. C.
1	1	CDR H. L. Murphy, Room 211, Federal Office Building, San Francisco

DISTRIBUTION LIST (Cont'd)

No. of Activities	Total Copies	
1	1	LCDR W. H. Bannister, CEC, USN, Field Command, Defense Atomic Support Agency, Sandia Base, Albuquerque, N. M.
1	1	Major Robert Crawford, USAF, Air Force Weapons Laboratory, Kirtland Air Force Base, Albuquerque, N. M.
1	1	Dr. John Balloch, Director, Operations Analysis, 26th Air Division, SAGE, Hancock Field, Syracuse, N. Y.
1	1	Mr. J. F. Tamanini, A & E Development Division, Office of Civil Defense, Department of Defense, Washington, D. C.
1	1	LCDR C. R. Whipple, CEC, USN, U. S. Naval Ordnance Laboratory, White Oak, Md.
1	1	Dr. W. E. Fisher, Air Force Weapons Laboratory, Kirtland Air Force Base, Albuquerque, N. M.
1	1	Mr. Everitt P. Blizzard, Director, Neutron Physics, Oak Ridge National Laboratory, P. O. Box X, Oak Ridge, Tenn.
1	1	LT M. MacDonald, CEC, USN, U. S. Naval School, CEC Officers, Port Hueneme, Calif.
1	1	Library, Engineering Department, University of California, 405 Hilgard Avenue, Los Angeles
1	1	Sandia Corporation, Box 5800, Albuquerque, N. M.
1	1	Rivers and Harbor Library, Princeton University, Princeton, N. J.
1	1	Head, Civil Engineering Department, Carnegie Institute of Technology, Schenley Park, Pittsburgh, Pa.
1	1	Mr. G. H. Albright, Head, Department of Architectural Engineering, 101 Engineering "A" Bldg., The Pennsylvania State University, University Park, Pa.
1	1	Dr. A. F. Dill, Civil Engineering Hall, University of Illinois, Urbana, Ill.
1	1	Dr. N. M. Newmark, Civil Engineering Hall, University of Illinois, Urbana, Ill.
1	1	Professor J. Neils Thompson, Civil Engineering Department, University of Texas, Austin, Tex.
1	1	Mr. Fred Sauer, Physics Department, Stanford Research Institute, Menlo Park, Calif.
1	1	Dr. T. H. Schiffman, Armour Research Foundation of Illinois, Institute of Technology, Technology Center, Chicago, Ill.
1	1	Dr. Robert V. Whitman, Massachusetts Institute of Technology, Cambridge, Mass.
1	1	Dr. Lewis V. Spencer, Ottawa University, Physics Department, Ottawa, Kan.
1	1	Mr. E. E. Shalowitz, Protective Construction, GSA Building, 19th and F Streets, N. W., Washington, D. C.

DISTRIBUTION LIST (Cont'd)

No. of Activities	Total Copies	
1	1	Mr. Werner Weber, Nuclear Engineering Consultant, N. Y. State Civil Defense Commission, P. O. Box 7007, State Office Building, Albany, N. Y.
1	1	Dr. Harold Brode, The Rand Corporation, 1700 Main Street, Santa Monica, Calif.
1	1	Mr. R. D. Cavanaugh, Barry Controls, Inc., 700 Pleasant Street, Watertown, Mass.
1	1	Mr. Kenneth Kaplan, Broadview Research Corporation, 1811 Trousdale Drive, Burlingame, Calif.
1	1	Mr. Thomas Morrison, American Machine and Foundry Company, 7501 North Natchez Avenue, Niles, Ill.
1	1	Mr. Walter Gunther, The Mitre Corporation, P. O. Box 208, Lexington, Mass.
1	1	Mr. W. R. Perret - 5112, Applied Experiments Division, Sandia Corporation, Albuquerque, N. M.
1	1	Mr. Lyndon Welch, Eberle M. Smith Associates, Inc., 153 East Elizabeth Street, Detroit, Mich.
1	1	Professor Herbert M. Bosch, Public Health Engineering, School of Public Health, University of Minnesota, Minneapolis, Minn.
1	1	Dr. Merit P. White, Civil Engineering Department, School of Engineering, University of Massachusetts, Amherst, Mass.
1	1	Dr. Robert J. Hansen, Department of Civil & Sanitary Engineering, Massachusetts Institute of Technology, Cambridge, Mass.
1	1	Mr. Harold Horowitz, Building Research Institute, National Academy of Sciences, 2101 Constitution Avenue, N. W., Washington, D. C.
1	1	Mr. Luke Vortman - 5112, Applied Experiments Division, Sandia Corporation, Albuquerque, N. M.
1	1	Mr. Richard Park, National Academy of Sciences, 2101 Constitution Avenue, N. W., Washington, D. C.
1	1	Mr. Frederick A. Pawley, AIA Research Secretary, American Institute of Architects, 1735 New York Avenue, N. W., Washington, D. C.
1	1	Dr. E. E. Massey, Defense Research Board, Department of National Defense, Ottawa, Canada
1	1	Dr. Robert Rapp, The Rand Corporation, 1700 Main Street, Santa Monica, Calif.
1	1	Dr. Stephen B. Withey, Program Director, Survey Research Center, University of Michigan, Ann Arbor, Mich.
1	1	Dr. Eric T. Clarke, Technical Operations, Inc., Burlington, Mass.
1	1	Dr. A. B. Chilton, Civil Engineering Hall, University of Illinois, Urbana, Ill.
1	1	Mrs. Shea Valley, CRTZS, A. F. Cambridge Research Center, L. G. Hanscom Field, Bedford, Mass.
1	1	Dr. J. T. Hanley, Department of Civil Engineering, University of Minnesota, Minneapolis, Minn.

DISTRIBUTION LIST (Cont'd)

No. of Activities	Total Copies	
1	1	Professor J. Silverman, Department of Chemical Engineering, University of Maryland, College Park, Md.
1	1	Dr. F. T. Mavis, Dean, College of Engineering, University of Maryland, College Park, Md.
1	1	Dr. Raymond R. Fox, Associate Professor and Director, Protective Construction Courses, The George Washington University, Washington, D. C.
1	1	Professor M. L. P. Go, Civil Engineering Department, University of Hawaii, Honolulu, Hawaii
1	1	Dr. James P. Romualdi, Department of Civil Engineering, Carnegie Institute of Technology, Pittsburg, Pa.
1	1	Dr. Nicholas Perrone, Structural Mechanics Branch, Office of Naval Research, Department of the Navy, Washington, D. C.
1	1	Dr. Aleksandar Sedmak Vesic, Associate Professor, Georgia Institute of Technology, Atlanta, Georgia
1	1	Mr. C. C. Mow, The Rand Corporation, 1700 Main Street, Santa Monica, Calif.
1	1	Systems Engineering Group, Deputy for Systems Engineering, Directorate of Technical Publications and Specifications, Wright-Patterson AFB, Ohio
1	1	Professor R. K. Watkins, Head Mechanical Engineering Department, Utah State University, Logan, Utah
1	1	Professor Don Linger, Department of Civil Engineering, University of Arizona, Tucson, Ariz.
1	1	Professor George Triandifilidis, University of New Mexico, Air Force Shock Tube Facility, P. O. Box 188, University Station, Albuquerque, N. M.
1	1	Professor Ulrich Luscher, Department of Civil and Sanitary Engineering, Massachusetts Institute of Technology, Cambridge, Mass.
1	1	Dr. M. T. Davison, Department of Civil Engineering, University of Illinois, Urbana, Ill.
1	1	Library, Department of Civil Engineering, University of Hawaii, Honolulu

U. S. Naval Civil Engineering Laboratory  
Technical Report R-332  
STATIC AND BLAST LOADING OF SMALL  
BURIED CYLINDERS, by J. R. Allgood and  
H. L. Gill  
74 p. illus 10 Nov 64 UNCLASSIFIED

To gain information which will serve as a guide in developing design methods for underground structures, continuous cylinders of shallow burial were subjected to static and blast loads. Data on the time and space variations of deflection, thrust, and moment and on the influence of a low-strength isolation material over the crown were obtained. The results show that (a) the use of such isolation material is of questionable benefit, (b) the deflection of the crown was much larger under blast loading than under static loading, and (c) the net arching over a shallow-buried cylinder in a uniform dry sand is essentially zero.

1. Structural tests — Buried cylinders
2. Shelters — Buried cylinders
- I. Allgood, J. R.
- II. Gill, H. L.
- III. Y-F008-08-02-108
- IV. DASA-13.018

U. S. Naval Civil Engineering Laboratory  
Technical Report R-332  
STATIC AND BLAST LOADING OF SMALL  
BURIED CYLINDERS, by J. R. Allgood and  
H. L. Gill  
74 p. illus 10 Nov 64 UNCLASSIFIED

To gain information which will serve as a guide in developing design methods for underground structures, continuous cylinders of shallow burial were subjected to static and blast loads. Data on the time and space variations of deflection, thrust, and moment and on the influence of a low-strength isolation material over the crown were obtained. The results show that (a) the use of such isolation material is of questionable benefit, (b) the deflection of the crown was much larger under blast loading than under static loading, and (c) the net arching over a shallow-buried cylinder in a uniform dry sand is essentially zero.

1. Structural tests — Buried cylinders
2. Shelters — Buried cylinders
- I. Allgood, J. R.
- II. Gill, H. L.
- III. Y-F008-08-02-108
- IV. DASA-13.018

U. S. Naval Civil Engineering Laboratory  
Technical Report R-332  
STATIC AND BLAST LOADING OF SMALL  
BURIED CYLINDERS, by J. R. Allgood and  
H. L. Gill  
74 p. illus 10 Nov 64 UNCLASSIFIED

To gain information which will serve as a guide in developing design methods for underground structures, continuous cylinders of shallow burial were subjected to static and blast loads. Data on the time and space variations of deflection, thrust, and moment and on the influence of a low-strength isolation material over the crown were obtained. The results show that (a) the use of such isolation material is of questionable benefit, (b) the deflection of the crown was much larger under blast loading than under static loading, and (c) the net arching over a shallow-buried cylinder in a uniform dry sand is essentially zero.

1. Structural tests — Buried cylinders
2. Shelters — Buried cylinders
- I. Allgood, J. R.
- II. Gill, H. L.
- III. Y-F008-08-02-108
- IV. DASA-13.018

U. S. Naval Civil Engineering Laboratory  
Technical Report R-332  
STATIC AND BLAST LOADING OF SMALL  
BURIED CYLINDERS, by J. R. Allgood and  
H. L. Gill  
74 p. illus 10 Nov 64 UNCLASSIFIED

To gain information which will serve as a guide in developing design methods for underground structures, continuous cylinders of shallow burial were subjected to static and blast loads. Data on the time and space variations of deflection, thrust, and moment and on the influence of a low-strength isolation material over the crown were obtained. The results show that (a) the use of such isolation material is of questionable benefit, (b) the deflection of the crown was much larger under blast loading than under static loading, and (c) the net arching over a shallow-buried cylinder in a uniform dry sand is essentially zero.

1. Structural tests — Buried cylinders
2. Shelters — Buried cylinders
- I. Allgood, J. R.
- II. Gill, H. L.
- III. Y-F008-08-02-108
- IV. DASA-13.018

Unclassified

Security Classification

DOCUMENT CONTROL DATA - R&D		
<i>(Security classification of title, body of abstract and indexing annotation must be entered when the overall report is classified)</i>		
1. ORIGINATING ACTIVITY (Corporate author) U. S. Naval Civil Engineering Laboratory Port Hueneme, California		2a. REPORT SECURITY CLASSIFICATION Unclassified
		2b. GROUP
3. REPORT TITLE STATIC AND BLAST LOADING OF SMALL BURIED CYLINDERS		
4. DESCRIPTIVE NOTES (Type of report and inclusive dates) Task phase December 1962-January 1963		
5. AUTHOR(S) (Last name, first name, initial) Allgood, J. R. Gill, H. L.		
6. REPORT DATE 10 November 1964	7a. TOTAL NO. OF PAGES 74	7b. NO. OF REFS 8
8a. CONTRACT OR GRANT NO. DASA 13,018	9a. ORIGINATOR'S REPORT NUMBER(S) TR 332	
b. PROJECT NO. Y-F008-08-02-108	9b. OTHER REPORT NO(S) (Any other numbers that may be assigned this report)	
c.		
d.		
10. AVAILABILITY/LIMITATION NOTICES Qualified requestors may obtain copies of this report from DDC.		
11. SUPPLEMENTARY NOTES	12. SPONSORING MILITARY ACTIVITY BuDocks-DASA	
13. ABSTRACT  To gain information which will serve as a guide in developing design methods for underground shelters, shallow-buried cylinders were subjected to static and dynamic loads. Data were obtained on the time and space variations of deflection, thrust, and moment and on the influence of a low-strength isolation material over the crown.		

DD FORM 1473 0101-807-6800  
1 JAN 64Unclassified  
Security Classification

14. KEY WORDS	LINK A		LINK B		LINK C	
	ROLE	WT	ROLE	WT	ROLE	WT
Research	8					
Testing	8					
Static tests	9					
Dynamic tests	9					
Subsurface structures	9		9			
Cylinders	9		9			
Structural analysis	9		9			
Dynamic structural analysis	9		9			
Static structural analysis	9		9			
Loads (forces)	9		9			
Deflection	9		9			
Moment	9		9			
Thrust	9		9			

INSTRUCTIONS

1. **ORIGINATING ACTIVITY:** Enter the name and address of the contractor, subcontractor, grantee, Department of Defense activity or other organization (*corporate author*) issuing the report.

2a. **REPORT SECURITY CLASSIFICATION:** Enter the overall security classification of the report. Indicate whether "Restricted Data" is included. Marking is to be in accordance with appropriate security regulations.

2b. **GROUP:** Automatic downgrading is specified in DoD Directive 5200.10 and Armed Forces Industrial Manual. Enter the group number. Also, when applicable, show that optional markings have been used for Group 3 and Group 4 as authorized.

3. **REPORT TITLE:** Enter the complete report title in all capital letters. Titles in all cases should be unclassified. If a meaningful title cannot be selected without classification, show title classification in all capitals in parenthesis immediately following the title.

4. **DESCRIPTIVE NOTES:** If appropriate, enter the type of report, e.g., interim, progress, summary, annual, or final. Give the inclusive dates when a specific reporting period is covered.

5. **AUTHOR(S):** Enter the name(s) of author(s) as shown on or in the report. Enter last name, first name, middle initial, if military, show rank and branch of service. The name of the principal author is an absolute minimum requirement.

6. **REPORT DATE:** Enter the date of the report as day, month, year, or month, year. If more than one date appears on the report, use date of publication.

7a. **TOTAL NUMBER OF PAGES:** The total page count should follow normal pagination procedures, i.e., enter the number of pages containing information.

7b. **NUMBER OF REFERENCES:** Enter the total number of references cited in the report.

8a. **CONTRACT OR GRANT NUMBER:** If appropriate, enter the applicable number of the contract or grant under which the report was written.

8b, 8c, & 8d. **PROJECT NUMBER:** Enter the appropriate military department identification, such as project number, subproject number, system numbers, task number, etc.

9a. **ORIGINATOR'S REPORT NUMBER(S):** Enter the official report number by which the document will be identified and controlled by the originating activity. This number must be unique to this report.

9b. **OTHER REPORT NUMBER(S):** If the report has been assigned any other report numbers (*either by the originator or by the sponsor*), also enter this number(s).

10. **AVAILABILITY/LIMITATION NOTICES:** Enter any limitations on further dissemination of the report, other than those

imposed by security classification, using standard statements such as:

- (1) "Qualified requesters may obtain copies of this report from DDC."
- (2) "Foreign announcement and dissemination of this report by DDC is not authorized."
- (3) "U. S. Government agencies may obtain copies of this report directly from DDC. Other qualified DDC users shall request through \_\_\_\_\_."
- (4) "U. S. military agencies may obtain copies of this report directly from DDC. Other qualified users shall request through \_\_\_\_\_."
- (5) "All distribution of this report is controlled. Qualified DDC users shall request through \_\_\_\_\_."

If the report has been furnished to the Office of Technical Services, Department of Commerce, for sale to the public, indicate this fact and enter the price, if known.

11. **SUPPLEMENTARY NOTES:** Use for additional explanatory notes.

12. **SPONSORING MILITARY ACTIVITY:** Enter the name of the departmental project office or laboratory sponsoring (*paying for*) the research and development. Include address.

13. **ABSTRACT:** Enter an abstract giving a brief and factual summary of the document indicative of the report, even though it may also appear elsewhere in the body of the technical report. If additional space is required, a continuation sheet shall be attached.

It is highly desirable that the abstract of classified reports be unclassified. Each paragraph of the abstract shall end with an indication of the military security classification of the information in the paragraph, represented as (TS), (S), (C), or (U).

There is no limitation on the length of the abstract. However, the suggested length is from 150 to 225 words.

14. **KEY WORDS:** Key words are technically meaningful terms or short phrases that characterize a report and may be used as index entries for cataloging the report. Key words must be selected so that no security classification is required. Identifiers, such as equipment model designation, trade name, military project code name, geographic location, may be used as key words but will be followed by an indication of technical context. The assignment of links, roles, and weights is optional.